Experimental Research

ANNALS OF MEDICINE & SURGERY

OPEN

Exploring the mechanism of Si-Ni-San against depression by UPLC-Q-TOF-MS/MS integrated with network pharmacology: experimental research

Keke Jia, PhD[a,b], Changyin Li, PhD[b], Meijuan Xu, PhD[b], Guoliang Dai, PhD[b], Jinyong Zhou, PhD[c], Biqing Chen, PhD[c], Jiandong Zou, PhD[b], Jia Li, PhD[a], Qingyu Zhang, PhD[a,*], Wenzheng Ju, PhD[b,*]

Background: Depression is becoming an urgent mental health problem. Si-Ni-San has been widely used to treat depression, yet its underlying pharmacological mechanism is poorly understood. Thus, we aim to explore the antidepressant mechanism of Si-Ni-San by chemical analysis and in-silico methods.

Methods: Compounds in Si-Ni-San were determined by ultra-high performance liquid chromatography coupled with quadrupole time-of-flight tandem mass spectrometry (UPLC-Q-TOF-MS/MS). Then, bioactive compounds were obtained from Traditional Chinese Medicines for Systems Pharmacology Database and Analysis Platform and SwissADME, and the potential targets of which were acquired from SwissTargetPrediction. Depression-related targets were collected from GeneCards. The intersection between compound-related targets and depression-related targets were screened out, and the overlapped targets were further performed protein-protein interaction, biological functional and pathway enrichment analysis. Finally, networks of Si-Ni-San against depression were constructed and visualized by Cytoscape.

Results: One hundred nineteen compounds in Si-Ni-San were determined, of which 24 bioactive compounds were obtained. Then, 137 overlapped targets of Si-Ni-San against depression were collected. AKT1, PIK3R1, PIK3CA, mTOR, MAPK1 and MAPK8 were the key targets. Furthermore, PI3K-Akt signalling pathway, serotonergic synapse, MAPK signalling pathway and neurotrophin signalling pathway were involved in the antidepressant mechanism of Si-Ni-San. It showed that components like sinensetin, hesperetin, liquiritigenin, naringenin, quercetin, albiflorin and paeoniflorin were the mainly key active compounds for the antidepressant effect of Si-Ni-San.

Conclusions: This study demonstrated the key components, key targets and potential pharmacological mechanisms of Si-Ni-San against depression. These results indicate that Si-Ni-San is a promising therapeutic approach for treatment of depression, and may provide evidence for the research and development of drugs for treating depression.

Keywords: depression, network pharmacology, Si-Ni-San, UPLC-Q-TOF-MS/MS

Introduction

Depression is the most prevalent mental disorder worldwide, with more than 264 million people suffering from the Global Burden of Diseases, Injuries, and Risk Factors Study 2017[1]. It is considered as a complicated neurodegenerative disease that is associated with dysfunction of the hypothalamic-pituitary-adrenal axis, lack of neurotransmitters, inflammation, impaired neuro-plasticity and neurogenesis, dysbiosis of microbiome and so on[2–4]. The current clinical first-line therapeutic drugs against depression are mainly selective serotonin reuptake inhibitors like fluoxetine, citalopram, escitalopram, paroxetine and sertraline, which are acting on a single target with some adverse effect[5]. It must evaluate the potential treatment effects by the risk–benefit analysis. Thus, the drug therapies with multiple actions and targets would show good efficacy and safety for the treatment of depression[6,7].

HIGHLIGHTS

- Exploring the antidepressant mechanism of Si-Ni-San by UPLC-Q-TOF-MS/MS integrated with network pharmacology.
- Key targets for the antidepressant effect of Si-Ni-San include AKT1, PIK3R1, PIK3CA, mTOR, MAPK1 and MAPK8.
- Sinensetin, hesperetin, liquiritigenin, naringenin, quercetin, albiflorin and paeoniflorin are the mainly key active compounds for the antidepressant effect of Si-Ni-San.

[a]School of Medicine & Holistic Integrative Medicine, Nanjing University of Chinese Medicine, [b]Department of Clinical Pharmacology and [c]Central Laboratory, Jiangsu Province Hospital of Chinese Medicine, Affiliated Hospital of Nanjing University of Chinese Medicine, Nanjing, P. R. China

Sponsorships or competing interests that may be relevant to content are disclosed at the end of this article

*Corresponding authors. Address: Affiliated Hospital of Nanjing University of Chinese Medicine, Nanjing 210029, Jiangsu, P. R. China. Tel./Fax: +25 865 878 07. E-mail: wzhju333@163.com (W. Ju), and Nanjing University of Chinese Medicine, Nanjing 210023, Jiangsu, P. R. China. Tel./Fax: +25 85811561. E-mail: zqy@njucm.edu.cn (Q. Zhang).

Annals of Medicine & Surgery (2024) 86:172–189

Received 1 August 2023; Accepted 21 October 2023

Published online 7 November 2023

http://dx.doi.org/10.1097/MS9.0000000000001464

Traditional Chinese medicine (TCM) has been used to treat depression with good efficacy and safety in clinic for many years[8]. However, these TCM formulas contain complex compounds and meanwhile act on multiple targets, making their underlying antidepressant mechanisms elusive. In the theory of TCM, the perspective of holism has long been central to herbal treatments for various diseases. It gives us a hint that understanding the scientific basis of TCM formulas at the molecular level needs from a systematic perspective. Network pharmacology is an interdisciplinary discipline newly developed in the systematic research of drugs based on artificial intelligence and Big Data, which matches well with the theory of TCM[9]. Moreover, with the fast-growing development of network pharmacology, a variety of in-silico methods have been used to clarify the potential pharmacological actions of TCM for the treatment of neurodegenerative diseases[10,11]. Through these in-silico methods, investment of human labour, materials and financial resources are reduced, facilitating understanding of pharmacological mechanisms for TCMs with known clinical therapeutic effect on some complex diseases as well.

Si-Ni-San is a classic TCM prescription, composed of Radix Bupleuri (*Bupleurum chinense DC.*), Fructus Aurantii Immaturus (*Citrus aurantium L.*), Radix Paeoniae Alba (*Paeonia lactiflora Pall.*) and Radix Glycyrrhizae (*Glycyrrhiza uralensis Fisch.*). It has been used to treat depression in clinical[12] and pre-clinical studies[13–15]. For example, Si-Ni-San is reported to show antidepressant action in chronic unpredictable mild stress (CUMS) mice[13]. Si-Ni-San also exhibits anti-depressive effect accompanied by improving synaptic plasticity in maternal separation-combined young-adult CUMS rats[14]. In our previous study, Si-Ni-San showed anti-depressive-like effect in reserpine-induced depressive rats[15]. Although these studies have revealed the antidepressant effect of Si-Ni-San, the underlying pharmacological mechanism is poorly understood.

Network pharmacology-based study is employed to clarify the molecular mechanism of Si-Ni-San formula for the application in nervous and mental diseases. However, compounds contained in Si-Ni-San are collected from Traditional Chinese Medicines for Systems Pharmacology Database and Analysis Platform (TCMSP), NCBI PubChem database, and wide-scale literature mining, instead of actual determined by related instruments and equipment[16]. In that way, it may be lack of reliability and accuracy for the actual antidepressant mechanism of Si-Ni-San. Only a few studies use actual determined components to clarify the possible mechanism of TCM by the method of network pharmacology[17,18]. Besides, In the modern pharmacological studies of TCM, ultra-high performance liquid chromatography coupled with quadrupole time-of-flight tandem mass spectrometry (UPLC-Q-TOF-MS/MS) method is often used to detect the actual components of TCM formulas, such as Si-Ni-San[19]. Hence, this study aimed to explore the potential mechanism of Si-Ni-San in the treatment of depression based on the strategy of UPLC-Q-TOF-MS/MS integrated with network pharmacology.

Materials and methods

Design of the study

This study was met the standards of Network Pharmacology Evaluation Method Guidance, which was mainly drafted by Prof. Shao Li of Tsinghua University[20]. The qualitative analysis of components in Si-Ni-San was carried out by UPLC-Q-TOF-MS/MS. Based on the actual determined components, network pharmacology was conducted for exploring the antidepressant mechanism of Si-Ni-San. First, the candidate bioactive components of Si-Ni-San were collected by absorption, distribution, metabolism and excretion (ADME) screening. Then, bioactive compounds-related targets of Si-Ni-San and depression-related targets were obtained. Subsequently, the overlapped targets between bioactive compounds-related targets of Si-Ni-San and depression-related targets were collected, which were considered as the potential targets for Si-Ni-San against depression. To figure out the relationships between these overlapped targets, protein-protein interaction (PPI) analysis was employed and visualized by Cytoscape software. In order to further clarify the specific antidepressant mechanism of Si-Ni-San, the above overlapped targets were carried out by Gene Ontology (GO) and Kyoto Encyclopedia of Genes and Genomes (KEGG) pathway enrichment analysis. Finally, the antidepressant mechanism of Si-Ni-San were analyzed and visualized in the way of some networks.

Preparation of Si-Ni-San

Si-Ni-San was composed of Radix Bupleuri, Fructus Aurantii Immaturus, Radix Paeoniae Alba and Radix Glycyrrhizae. Each herb was used as an amount of 20 g. All these herbs were purchased from Jiangsu Province Hospital of Chinese Medicine. The crude herbs were pre-immersed in eight times volumes of distilled water for 0.5 h and decocted for 0.5 h. Then, the supernatants were collected by filtering through eight-layers of gauze. After removal of the supernatants, the rest was added with six times volumes of distilled water and boiled twice for 0.5 h. Meanwhile, the two supernatants were collected by filtering through eight-layers of gauze. Those three supernatants were merged and condensed into extractum by rotary evaporators at a temperature of 60°C. Finally, the extractum was stored at −20°C for future use.

Analysis of compound profiles of Si-Ni-San by UPLC-Q-TOF-MS/MS

The qualitative analysis of components in water extract of Si-Ni-San was employed by method of UPLC-Q-TOF-MS/MS. 1 g of Si-Ni-San extract was dissolved in 25 ml distilled water. Then, it was centrifuged twice at 12 000*g* for 5 min to get the supernatant. The supernatant was subsequently filtered through a 0.22 μm membrane before analysis. Chromatographic separation was performed on a series of 1290 HPLC system (Agilent). The HPLC system was equipped with an Agilent SB-C18 column (4.6 × 100 mm, 1.8 μm). Ultrapure water containing 0.1% formic acid (v/v, A) and acetonitrile/methanol (v/v, 1:1, B) were used as the mobile phase. The flow rate was set at 0.4 ml/min. The mobile phase was employed by a gradient elution manner as follows: 0–2.5 min, 15%→20%B; 2.5–7 min, 20%→25%B; 7–12 min, 25%→50%B; 12–19 min, 50%→80%B; 19–23 min, 80%→46%B; 23–26 min, 46%→15%B; 26–30 min, 15%B. The column oven temperature was maintained at 40°C. The injection volume for sample was 5 μl. The Triple TOF 5600 (AB SCIEX) equipped with electron spray ionization source was used for MS detection. Both positive and negative ion modes were carried out. The ion spray voltage floating was set at 5500 V for positive ion mode, and 4500 V for negative ion mode, respectively. TOF/MS scan conditions were as follows. TOF mass range was set at m/z

100–1300 Da for positive ion mode and m/z 50–1300 Da for negative ion mode, respectively. Declustering potential was set at 80 V. Collision energy was set at 10 eV. Ion source gas 1 was set at 50 psi and ion source gas 2 was set at 60 psi. Curtain gas was set at 20 psi. Heater temperature was set at 600°C. Accumulation time was set at 0.25 s. The options of IDA, DBS and high sensitivity were chosen. Major IDA switch criteria were as follows: Intensity exceeds 100 cps, exclusion isotope within 4 Da, mass tolerance 50 mDa, maximum number of candidate ions to monitor per cycle 10. For Product Ion scan type, TOF mass range was set at m/z 100–1300 Da for positive ion mode and m/z 50–1300 Da for negative ion mode, respectively. Collision voltage set at 30 ± 15 eV. The other parameters were the same with TOF/MS scan type. All the operations and acquisition were controlled by Analyst® TF 1.6 software (AB SCIEX, Foster City, CA). Data like m/z, retention time (RT) and ion intensity of the typical ions were obtained using the XIC manager of Peak view software 1.2.0 (AB SCIEX, Foster City, CA). MS and MS/MS information of components in Si-Ni-San were referred to some standards, online servers and databases like PubChem (https://pubchem.ncbi.nlm.nih.gov/), The Human Metabolome Database (HMDB, https://hmdb.ca/)[21], MassBank of North America (MoNA, https://mona.fiehnlab.ucdavis.edu/), RIKEN tandem mass spectral database (ReSpect, http://spectra.psc.riken.jp/)[22], SciFinder (https://scifinder.cas.org), and some references for further confirmation[19,23–32]. Eventually, details like CAS number, 3D molecular structure files, simplified molecular input line entry specification (SMILES) information of these compounds were collected for future target prediction.

Collection of candidate bioactive phytochemicals of Si-Ni-San

These above qualitative compounds of Si-Ni-San were further identified by ADME screening from Traditional Chinese Medicine Systems Pharmacology Database and Analysis Platform (TCMSP, https://lsp.nwu.edu.cn/)[33]. Compounds with oral bioavailability (OB) ≥ 30% and drug-likeness (DL) ≥ 0.18 were considered as candidate bioactive compounds. This criteria for screening was referred to a previous study[34]. For those compounds without detailed information from TCMSP, SwissADME (http://www.swissadme.ch) was employed to predict ADME parameters and evaluate pharmacokinetics and drug-likeness of small molecules[35]. Compounds meeting at least two of five features of drug-likeness (Lipinski, Ghose, Veber, Egan and Muegge) and high gastrointestinal absorption were selected as candidates from SwissADME.

Prediction of the bioactive compounds-related targets

Potential targets of active compounds were obtained from SwissTargetPrediction (http://www.swisstargetprediction.ch/), which was a popular online server providing the most probable macromolecular targets of a small molecule[36]. Three-dimensional molecular structure files of each ingredient were acquired from PubChem. Then these structure files were imported into SwissTargetPrediction to get the compounds-related targets. Targets with probability ≥ 0.1 were chosen as potential human targets in this study. All the targets obtained above were standardized as gene names and UniProt IDs by searching from Uniprot KB (https://www.uniprot.org/) database with a "Homo sapiens" filter.

Collection of depression- related targets

Depression-related targets were collected from GeneCards (https://www.genecards.org/), which was a database integrating all annotated and predicted genes associated to human diseases[37]. The keywords of "depression", "depressive syndrome", "major depression" and "major depressive disorder" were used to search depression-associated targets. These protein-coding genes were selected with relevance score over than twice the median score. Relevance score values of "depression", "depressive syndrome", "major depression", "major depressive disorder" over than 4.12, 9.70, 5.64 and 13.26 were selected, respectively. All the targets obtained above were standardized as gene names and UniProt IDs by searching from Uniprot KB (https://www.uniprot.org/) database with a "Homo sapiens" filter. Then, shared targets collected from these four keywords were screened out for further analysis.

Intersection of bioactive compounds-related targets of Si-Ni-San and depression- related targets

The putative target genes of Si-Ni-San were mapped to the depression-related target genes. Then, the intersection between compounds-related targets and depression-related targets were screened out. The selected targets were visualized by a Venn diagram (https://bioinfogp.cnb.csic.es/tools/venny/). The overlapped targets were considered as potential targets for Si-Ni-San against depression. The bioactive components and their putative targets were used to establish the compound-target network. Finally, the visualization of the established network was carried out by Cytoscape software (https://cytoscape.org/).

Protein-protein interactions

The PPI network of potential targets for Si-Ni-San against depression was constructed by STRING database (https://string-db.org/). This database was aimed to collect, score and integrate all publicly available sources of protein-protein interaction information[38]. These targets were then imported into STRING and "Homo sapiens" filter was employed. High confidence score > 0.7 was set. All the disconnected nodes were hidden in this network. The extracted PPI data were input into Cytoscape software and analyzed with cytoHubba plugin. Eventually, the top 20 targets with higher degree level were considered as key targets for Si-Ni-San against depression.

GO and KEGG pathway enrichment analysis

Database for Annotation, Visualization and Integrated Discovery (DAVID) was a database for bioinformatics enrichment analysis (https://david.ncifcrf.gov/). It was employed for GO and KEGG enrichment analysis[39]. GO was composed of biological process (BP), cellular component (CC) and molecular function (MF). Specially, potential targets for Si-Ni-San against depression were input into DAVID. For analysis, terms with value of false discovery rate (FDR) < 0.01 were reserved. Finally, the top 10 GO terms and 20 KEGG pathways were plotted by a free online platform for analyzing and visualizing the results of GO and KEGG enrichment analysis (http://www.bioinformatics.com.cn).

Network construction

Three networks were constructed as follows: (1) compound-target network of Si-Ni-San was constructed by connecting chemical compounds with corresponding targets (C-T network); (2) compound-target-disease network of Si-Ni-San against depression (C-T-D network); (3) compound-target-pathway network of Si-Ni-San against depression (C-T-P network). These networks were constructed using the network visualization software of Cytoscape. Furthermore, Cytoscape was used to integrate and analyze the networks. Some parameters like "degree value" was calculated to evaluate the topological coefficients of each node, which represented the number of edges connected to a node in these networks.

Data analysis

For the qualitative analysis of components in Si-Ni-San, the found mass of a component and ion intensity of the typical ions were obtained using the XIC manager of Peak view software (Version 1.2.0). According to the traditional practice, the error between actual mass and found mass of a component was set at below ± 5 ppm for positive ion mode and ± 10 ppm for negative ion mode, respectively. High confidence score > 0.7 was set in the network of protein-protein interactions by a freely available database of STRING (Version 12.0, License 'Creative Commons BY 4.0'). FDR value < 0.01 was considered as significantly enriched in GO and KEGG analysis by a freely available database of DAVID (Version 6.8).

Results

Chemical analysis of Si-Ni-San

In this study, the typical total ion chromatograms (TICs) of Si-Ni-San water extract in negative (Fig. 1A) and positive ion modes (Fig. 1B) are obtained. 100 compounds were identified in negative ion mode (Table 1) and 61 compounds were identified in positive ion mode (Table 2) in water extract of Si-Ni-San. There were 119 compounds after removing the 42 duplicates both in negative and positive ion mode in Si-Ni-San (Supplementary Table 1, Supplemental Digital Content 1, http://links.lww.com/MS9/A290 Fig. 2A). Si-Ni-San mainly contained 39 flavonoids like 5-demethylnobiletin, 5-hydroxyauranetin, hesperetin, liquiritigenin, naringenin, quercetin and sinensetin, 33 triterpenoid saponins like saikosaponin A and saikosaponin D, 16 terpenoids like albiflorin, and paeoniflorin, and 16 organic acids like ferulic acid and gallic acid.

Candidate bioactive compounds and potential targets of Si-Ni-San

A total of 24 bioactive compounds were identified (Table 3), among them 21 compounds were screened out from TCMSP and 3 compounds were screened out from SwissADME. These active compounds were mainly contained 15 flavonoids and 6 terpenoids. Flavonoids include hesperetin, liquiritigenin, naringenin, quercetin, sinensetin, 5-demethylnobiletin and 5-hydroxyauranetin, and terpenoids include albiflorin and paeoniflorin and so on. Subsequently, putative targets of these constituents were acquired from SwissTargetPrediction database. Finally, a total of 1195 targets of 24 active compounds were predicted by SwissTargetPrediction (Supplementary Table 2 Supplemental Digital Content 1, http://links.lww.com/MS9/A290), and 412 potential compound-related targets were left after removing the duplicates (Supplementary Table 3 Supplemental Digital Content 1, http://links.lww.com/MS9/A290).

Targets of compounds in Si-Ni-San against depression

There were 2013 targets of "depression", 2478 targets of "depressive syndrome", 2222 targets of "major depression", 1916 targets of "major depressive disorder" from GeneCards database, respectively. Then 1061 shared depression-related targets were remained after screening (Supplementary Table 4, Supplemental Digital Content 1, http://links.lww.com/MS9/A290 Fig. 2B). Subsequently, the intersection between 412 potential compound-related targets and 1061 depression-related targets was performed. Finally, 137 overlapped targets between compound-related targets and depression-related targets, which were considered as potential targets for Si-Ni-San against depression were obtained (Supplementary Table 5, Supplemental Digital Content 1, http://links.lww.com/MS9/A290 Fig. 2C).

PPI network of targets for Si-Ni-San against depression

To further clarify the key regulatory targets of Si-Ni-San against depression, the above 137 potential targets were imported into the STRING database and analyzed by Cytoscape cytoHubba plugin. The PPI network was shown in Figure 3A. With the confidence score > 0.7, the PPI network was composed of 130 nodes and 746 edges, and average degree value was 11.48. In these nodes, 53 targets had a degree value over than the average value. The top 20 targets with higher levels of degree value were considered as core targets for Si-Ni-San in the treatment of depression, including serine/threonine-protein kinase (AKT1), mitogen-activated protein kinase 1 (MAPK1), phosphatidylinositol 3-kinase regulatory subunit alpha (PIK3R1), phosphatidylinositol-4,5-bisphosphate 3-kinase catalytic subunit alpha (PIK3CA), mitogen-activated protein kinase 8 (MAPK8) and mammalian target of rapamycin (mTOR) (Fig. 3B). Among them, AKT1, PIK3R1, PIK3CA are coding genes involved in PI3K-Akt signalling pathway, and mTOR is the downstream component of this pathway. MAPK1 and MAPK8 are coding genes of MAPK family participating in inflammation.

Biological function and pathway enrichment analysis

To explore the multiple functions of 137 potential antidepressant targets of Si-Ni-San, GO and KEGG pathway enrichment analysis were performed by DAVID database. In GO enrichment analysis, these 137 target genes were enriched in 130 biological process (BP), 40 cellular component (CC), and 35 molecular function (MF) (FDR < 0.01, Supplementary Table 6 Supplemental Digital Content 1, http://links.lww.com/MS9/A290). The top 10 GO functional categories in BP, CC and MF were presented in Figure 4. The top 3 BP terms were mainly enriched in response to drug (GO:0042493), positive regulation of ERK1 and ERK2 cascade (GO:0070374), and positive regulation of MAP kinase activity (GO:0043406). The top 3 CC terms were plasma membrane (GO:0005886), integral component of plasma membrane (GO:0005887), and dendrite (GO:0030425). The top 3 MF terms included enzyme binding (GO:0019899), drug binding (GO:0008144) and protein kinase activity (GO: 0004672). These 137 target genes were also

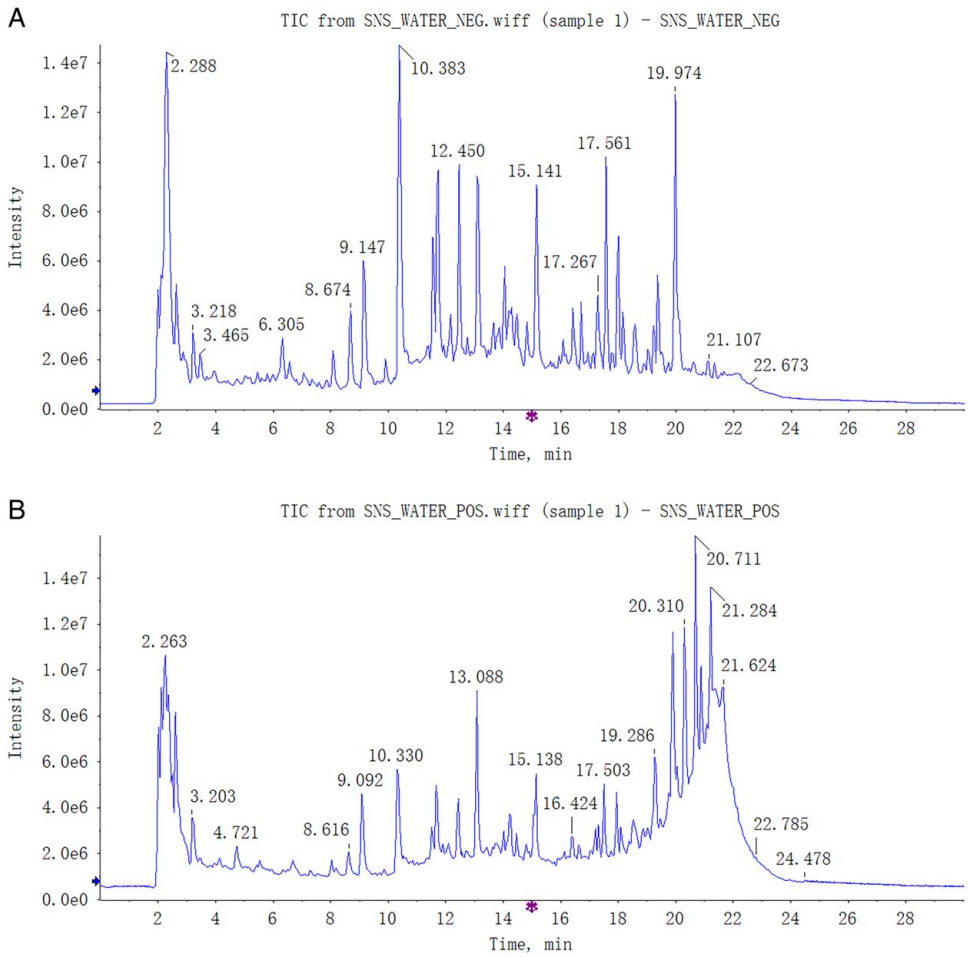

Figure 1. Typical total ion chromatograms (TICs) of Si-Ni-San water extract. (A) Negative ion mode was showed by UPLC-Q-TOF-MS/MS. (B) Positive ion mode was showed by UPLC-Q-TOF-MS/MS.

enriched in 86 pathways, which were predicated to participate in the antidepressant action of Si-Ni-San (FDR < 0.01, Supplementary Table 7 Supplemental Digital Content 1, http://links.lww.com/MS9/A290). The top 20 enriched pathways were shown as Figure 5. It showed that antidepressant effect of Si-Ni-San may involve regulation of PI3K-Akt signalling pathway (hsa04151), serotonergic synapse (hsa04726), MAPK signalling pathway (hsa04010) and neurotrophin signalling pathway (hsa04722).

Network construction and analysis

C-T network was first constructed. The C-T network included 437 nodes and 1219 edges, and its average degree value was 5.58 (Fig. 6). The bioactive ingredients were sorted according to the descending order of degree value. The top 10, including obacunon (degree = 111), 5-demethylnobiletin (degree = 104), 5-hydroxyauranetin (degree = 104), hesperetin (degree = 104), quercetin (degree = 104), sinensetin (degree = 104), liquiritigenin (degree = 102), naringenin (degree = 93), albiflorin (degree = 67) and paeoniflorin (degree = 61) were predicted to be the key ingredients in C-T network. Furthermore, the C-T-D network was constructed (Fig. 7). This network included 162 nodes and 577 edges, and its average degree value was 7.12. Similarly, the bioactive ingredients were sorted according to the descending order of degree value. The top 10 ingredients were obacunon (degree = 47), sinensetin (degree = 38), hesperetin (degree = 37), 5-demethylnobiletin (degree = 35), liquiritigenin (degree = 34), 5-hydroxyauranetin (degree = 33), naringenin (degree = 32), quercetin (degree = 31), albiflorin (degree = 26) and formononetin (degree = 23) in C-T-D network. Finally, C-T-P network was constructed (Fig. 8). It contained 135 nodes and 706 edges, and its average degree value was 10.46. The bioactive ingredients were also sorted according to the descending order of degree value. The top 10 ingredients were obacunon (degree = 33), sinensetin (degree = 28), hesperetin (degree = 27), 5-demethylnobiletin (degree = 26), 5-hydroxyauranetin (degree = 23), liquiritigenin (degree = 23), naringenin (degree = 22), quercetin (degree = 21), albiflorin (degree = 20) and paeoniflorin (degree = 15) in C-T-P network. Briefly, in the C-T, C-T-D, C-T-P networks, compounds of obacunon, sinensetin, hesperetin, 5-demethylnobiletin, 5-hydroxyauranetin, liquiritigenin, naringenin, quercetin, albiflorin and paeoniflorin were considered as key bioactive compounds for the antidepressant effect of Si-Ni-San.

Table 1

Identification of chemical compounds of Si-Ni-San in negative ion mode by UPLC-Q-TOF-MS/MS

No	tR (min)	Formula	Mass ion type	Found mass/error (Da, ppm)	Intensity	MS/MS ion type (m/z, area%)	Identification	Reference
1	2.27	$C_{12}H_{22}O_{11}$	$[M-H]^-$	341.10944 (1.5)	394 312	341.1101 (41.22), 179.0562 (14.02), 161.045 (3.86), 119.0346 (6.58), 89.0247 (10.81), 59.0154 (5.06)	Sucrose	[19]
2	2.62	$C_{16}H_{24}O_{10}$	$[M+HCOOH-H]^-$	421.13603 (4.7)	102 128	421.1371 (10), 375.131 (27.35), 345.1206 (28.24), 213.0772 (3.12), 195.0666 (5.54), 183.0661 (2.72), 165.0558 (5.18)	Desbenzoylpaeoniflorin	[23,30]
3	3.23	$C_4H_6O_4$	$[M-H]^-$	117.02019 (7.3)	14 078	117.0194 (18.97), 99.0088 (9.89), 73.0305 (59.11), 55.0198 (2.89)	Succinic acid	[22]
4	3.28	$C_{13}H_{16}O_{10}$	$[M-H]^-$	331.06772 (2)	22 542	331.0677 (34.03), 271.0478 (12.19), 232.874 (4.78), 211.0257 (5.31), 169.0145 (20.43), 125.0247 (4.99)	β-Glucogallin	[23]
5	3.46	$C_7H_6O_5$	$[M-H]^-$	169.01493 (4.1)	616 187	169.0144 (23.95), 125.0246 (48.13), 107.0142 (1.56), 97.0299 (2.39), 81.0354 (2.79), 79.0201 (7.03), 69.0359 (2.29)	Gallic acid	[21,23]
6	3.98	$C_8H_8O_5$	$[M-H]^-$	183.0305 (3.3)	8586	183.0291 (26.87), 139.0402 (7.81), 137.0094 (2.58), 124.0194 (2.46), 111.0485 (16.28), 93.0332 (6.39), 83.0517 (16.09)	Methyl gallate	[28]
7	4.7	$C_{16}H_{18}O_9$	$[M-H]^-$	353.08898 (3.3)	35 795	353.0887 (26.7), 191.0562 (36.49), 179.035 (19.79), 135.0452 (8.61)	Neochlorogenic acid	MoNA
8	5.17	$C_7H_6O_4$	$[M-H]^-$	153.02003 (4.6)	34 494	153.0187 (18.82), 109.0295 (52.23), 108.0208 (20.25), 91.0191 (2.65)	Protocatechuic acid	MoNA
9	5.35	$C_{27}H_{24}O_{18}$	$[M-H]^-$	635.09114 (3.4)	3808	635.0936 (50.65), 483.0825 (2.43), 465.0696 (13.11), 421.079 (1.42), 313.055 (3.42), 295.0475 (1.42), 169.0148 (1.98)	1,3,6-Trigalloyl glucose	[23]
10	5.45	$C_{23}H_{28}O_{12}$	$[M-H]^-$	495.15189 (2.2)	32 777	495.1528 (79.34), 333.1014 (1.5), 281.0677 (2.27), 137.0249 (11.04)	Oxypaeoniflorin	[23,28]
11	6.04	$C_{15}H_{14}O_6$	$[M-H]^-$	289.07233 (2)	12 189	289.0728 (32.36), 245.082 (9.1), 203.0721 (6.35), 151.0396 (2.54),125.0235 (3.03),123.0451 (3.05)	Catechin	[19,23]
12	6.32	$C_{26}H_{28}O_{14}$	$[M-H]^-$	563.1424 (3.1)	39 468	563.1454 (9.15), 443.0589 (1.01),353.0895 (9.61), 209.0459 (36.09), 191.0566 (5.77),165.0559 (32.44)	Isoschaftoside	MoNA
13	6.32	$C_9H_{10}O_3$	$[M-H]^-$	165.05669 (5.9)	569 503	165.0566 (61.45),147.0457 (1.17),121.0666 (11.7), 119.0503 (5.95),93.0354 (9.93),59.0158 (7.37)	Paeonol	[19]
14	6.34	$C_6H_8O_7$	$[M-H]^-$	191.02003 (1.6)	12 896	191.0191 (16.77), 129.0194 (1.81),111.0098 (8.75), 102.9487 (4.21), 87.0078 (2.68),85.0301 (16.79),67.019 (4.71),57.0352 (2.41)	Citric acid	[23]
15	6.47	$C_{16}H_{18}O_9$	$[M-H]^-$	353.08879 (2.8)	39 741	353.089 (17.69),191.0569 (18.02),179.0353 (18.86), 173.0457 (26.16),155.0347 (2.16),135.0458 (10.04)	Chlorogenic acid	MoNA
16	6.56	$C_{27}H_{32}O_{14}$	$[M-H]^-$	579.1729 (1.7)	56 762	579.1409 (3.55),417.1201 (61.78),255.0665 (27.32)	Liquiritigenin 7,4'-diglucoside	[29]
17	6.69	$C_{24}H_{30}O_{13}$	$[M-H]^-$	525.16257 (2.3)	45 545	525.1642 (71.71),495.1538 (2.26),363.1101 (1.79),167.0347 (14.13)	Mudanpioside E	[19,23,30]
18	7.34	$C_{29}H_{38}O_{16}$	$[M+HCOOH-H]^-$	687.21744 (6.3)	93 541	687.2191 (29.51),641.2143 (43.7),519.1751 (10.09), 475.1851 (2.01),445.1357 (1.35),121.0296 (3.5)	β-Gentiobiosylpaeoniflorin	[23]
19	7.42	$C_7H_6O_3$	$[M-H]^-$	137.02529 (6.3)	16 842	137.0237 (10.36),93.0352 (85),65.0417 (4.44)	4-Hydroxybenzoic acid	[23]
20	8.08	$C_{27}H_{30}O_{15}$	$[M-H]^-$	593.15427 (5.2)	629 264	593.1559 (69.89),473.1121 (8.88),383.0792 (3.95),353.0683 (5.65)	Lonicerin	[19]
21	8.17	$C_9H_6O_4$	$[M-H]^-$	177.02022 (5)	5083	177.0193 (59.66),149.0247 (3.94),133.0301 (12.6),105.0355 (5.33)	Esculetin	MoNA
22	8.22	$C_9H_8O_4$	$[M-H]^-$	179.0359 (5.1)	103 847	179.0355 (16.32),135.0458 (62.47),134.0379 (13.06),107.0508 (1.17)	Caffeic acid	[25]
23	8.67	$C_{29}H_{38}O_{16}$	$[M+HCOOH-H]^-$	687.21786 (6.9)	939 705	687.2194 (12.3),641.2138 (6.79),623.2034 (3.44),611.2022 (15.9), 593.1909 (33.26),489.1639 (5.3),471.1531 (4.51)	Isomaltopaeoniflorin	[19,30]
24	9.15	$C_{23}H_{28}O_{11}$	$[M-H]^-$	479.15709 (2.5)	36 411	479.158 (39.27),357.1198 (3.38),327.1096 (2.45),283.0832 (3.08), 195.0672 (1.95),121.0298 (39.38),77.041 (1.34)	Albiflorin*	Standard
25	10.2	$C_{26}H_{28}O_{14}$	$[M-H]^-$	563.1427 (3.7)	75 201	563.1454 (74.14),473.1113 (3.47),443.1013 (3.3),353.0679 (4.71)	Schaftoside	[19]
26	10.4	$C_{23}H_{28}O_{11}$	$[M-H]^-$	479.15757 (3.5)	165 990	479.1575 (15.93),449.1469 (20.87),357.1198 (2.59),327.1092 (13.09), 165.0549 (4.58),121.0294 (26.9),77.04 (1.41)	Paeoniflorin[a]	Standard
27	11.2	$C_{20}H_{20}O_8$	$[M-H]^-$	387.1092 (1.7)	19 758	387.1107 (44.5),343.1202 (7.71),341.1088 (2.5),249.0633 (2.46), 193.0511 (16.23),137.025 (3.84),134.0377 (7.09)	5-Hydroxyauranetin	[21]
28	11.2	$C_{27}H_{32}O_{15}$	$[M-H]^-$	595.16842 (2.6)	59 972	595.1702 (35.25),549.1562 (15.57),287.0567 (20.56), 254.053 (1.61),253.0527 (2.2),151.003 (2.84)	Eriocitrin	[22]
29	11.4	$C_{21}H_{22}O_9$	$[M-H]^-$	417.12013 (2.5)	118 023	417.121 (13.53),255.067 (70.93),135.0086 (8.03),119.0502 (4.36)	Neoliquiritin	[29]
30	11.5	$C_{26}H_{30}O_{13}$	$[M-H]^-$	549.16227 (1.7)	2E + 06	549.1623 (75.88),417.1196 (2.29),255.0657 (12.53),135.0087 (1.73)	Liquiritin apioside	[29]
31	11.6	$C_{25}H_{24}O_{12}$	$[M+HCOOH-H]^-$	561.12659 (4.8)	287 311	561.1282 (24),385.0782 (3.21),367.0682 (23.31),323.0776 (5.01), 193.0503 (11.06),173.0087 (5.72),129.0191 (6.4),85.0303 (4.81)	Isochlorogenic acid b	[19]
32	11.7	$C_{21}H_{22}O_9$	$[M-H]^-$	417.12077 (4)	3E + 06	417.1195 (12.89),255.0662 (68.85),135.0088 (9.88),119.0506 (3.43)	Liquiritin[a]	Standard
33	11.8	$C_{27}H_{30}O_{16}$	$[M-H]^-$	609.14856 (4)	40 101	609.1507 (79.97),301.0365 (4.2)	Rutin	MoNA
34	11.9	$C_{30}H_{32}O_{15}$	$[M-H]^-$	631.16881 (3.1)	279 673	631.17 (86.03),465.1404 (4.16),313.0565 (1.4)	Galloylalbiflorin	[30]
35	12.1	$C_{10}H_{10}O_4$	$[M-H]^-$	193.05134 (3.7)	125 906	193.0511 (16.56),178.0274 (23.26),149.0607 (6.15), 134.0378 (44.37),133.0298 (6.71)	Ferulic acid	[22,25]
36	12.2	$C_{30}H_{32}O_{15}$	$[M-H]^-$	631.16916 (3.7)	639 128	631.1709 (58.47),613.1614 (12.69),509.1331 (1.26),491.1224 (4.51), 479.1218 (1.01),399.0954 (2.74),313.0576 (3.57),271.0466 (3.39)	Galloylpaeoniflorin	[23,30]
37	12.3	$C_{25}H_{24}O_{12}$	$[M+HCOOH-H]^-$	561.12684 (5.3)	93 949	561.1296 (30.58),367.0693 (18.45),323.0784 (3.75),193.0516 (8.97), 173.0098 (4.26),129.0198 (5.46),85.0306 (3.93)	Isochlorogenic acid c	[19]
38	12.5	$C_{27}H_{32}O_{14}$	$[M-H]^-$	579.1736 (2.9)	3E + 06	579.1753 (29.63),295.0618 (3.54),271.0614 (51.19),151.0039 (3.42)	Naringin[a]	Standard
39	12.7	$C_{53}H_{86}O_{24}$	$[M+HCOOH-H]^-$	1151.55701 (7.8)	10 223	1151.5643 (12.41),1105.5585 (63.22),791.4335 (5.3)	Saikosaponin V	[19]
40	12.8	$C_{27}H_{30}O_{14}$	$[M-H]^-$	577.15804 (3)	44 658	577.1607 (50.46),492.1242 (1.13),269.0465 (41.55)	Rhoifolin	[22,25]
41	13	$C_{28}H_{32}O_{15}$	$[M-H]^-$	607.16957 (4.5)	28 703	607.1741 (21.67),561.1667 (4.31),545.1357 (2.06),505.1034(8.88), 463.0928 (5.37),301.0744 (3.61),299.0571 (15.64)	Diosmetin-7-neohesperidoside	MoNA
42	13.1	$C_{28}H_{34}O_{15}$	$[M-H]^-$	609.1857 (5.3)	2E + 06	609.1862 (21.97),325.0727 (2.87),301.0716 (53.79),286.0491 (1.73)	Hesperidin[a]	Standard
43	13.3	$C_{25}H_{24}O_{12}$	$[M+HCOOH-H]^-$	561.1274 (6.3)	174 797	561.1276 (25.84),367.0682 (22.87),323.0782 (4.33),193.0505 (8.06), 173.0089 (3.22),147.0295 (3.1),129.0195 (3.62),85.0295 (5.31)	Isochlorogenic acid a	[19]
44	13.4	$C_{23}H_{28}O_{11}$	$[M-H]^-$	479.15884 (6.2)	8623	479.1582 (23.12),357.1219 (2.78),121.0296 (16.57),77.0398 (1.37)	Mudanpioside I	[19,23]
45	13.6	$C_{28}H_{34}O_{15}$	$[M-H]^-$	609.18495 (4)	51 369	609.1868 (70.74),549.1643 (1.5),301.0726 (16.74)	Neohesperidin[a]	Standard
46	13.7	$C_{26}H_{30}O_{13}$	$[M-H]^-$	549.16335 (3.6)	496 508	549.1641 (61.75),417.1204 (1.8),255.0668 (24.9),135.0089 (2.08)	Isoliquiritin apioside	[29]
47	13.8	$C_7H_6O_2$	$[M-H]^-$	121.02997 (3.9)	14 043	121.0295 (23.38),92.0267 (1.02),77.0403 (74.22)	Benzoic acid	[23]
48	14	$C_{21}H_{22}O_9$	$[M-H]^-$	417.12062 (3.6)	2E + 06	417.121 (19.01),297.0778 (2.29),255.0667 (49.86), 148.0168 (6.62),135.0091 (7.96),119.0504 (1.52)	Isoliquiritin	[29]
49	14.2	$C_{23}H_{26}O_{10}$	$[M+HCOOH-H]^-$	507.1529 (6.3)	702 539	507.1539 (42.23),461.1484 (14.77),431.1376 (12.17),345.0639 (2.81), 339.1097 (6.18),177.0561 (4.93),121.0299 (6.94)	Lactiflorin	[23]
50	14.3	$C_{21}H_{22}O_9$	$[M-H]^-$	417.12064 (3.7)	81 974	417.1209 (15.89),255.0669 (66.07),135.0088 (7.52),119.0505 (3.41)	Neoisoliquiritin	[29]
51	14.4	$C_{21}H_{18}O_{11}$	$[M-H]^-$	445.07872 (2.4)	66 026	445.0801(16.58),269.0462(68.24),175.0241(3.27),113.0249(2.21)	Baicalin	MoNA
52	14.5	$C_{20}H_{22}O_7$	$[M-H]^-$	373.13042 (3.1)	65 476	373.1307(48.57),355.1198(2.12),327.1243(3.62), 179.0714(9.35),164.048(3.71),99.0088(2.04)	Epinortrachelogenin	[19]
53	14.6	$C_{16}H_{14}O_5$	$[M-H]^-$	285.07778 (3.3)	49 438	285.0776(28.04),270.0543(25.25),177.0203(3.01),150.0326(28.78)	Licochalcone B	[22]
54	14.8	$C_{15}H_{12}O_4$	$[M-H]^-$	255.06704 (3)	211 548	255.0662(27.39),135.0088(26.86),119.0503(36.11),91.0194(5.09)	Liquiritigenin	[24]
55	15.2	$C_{28}H_{34}O_{14}$	$[M-H]^-$	593.19031 (4.6)	559 632	593.1902(34.85),327.0881(2.31),309.0777(4.61),285.0773(50.97)	Poncirin	MoNA
56	15.3	$C_{15}H_{10}O_7$	$[M-H]^-$	301.03711 (5.8)	7399	301.0368(41.15),178.999(7.65),151.0035(15.22),121.0299(2.1)	Quercetin[a]	Standard
57	15.5	$C_{27}H_{32}O_{15}$	$[M-H]^-$	595.16974 (4.9)	10 217	595.1872(49.21),549.1675(2.8),387.1098(3.39),193.0521(2.4)	Neoeriocitrin	[19,22]
58	16.1	$C_{42}H_{64}O_{16}$	$[M-H]^-$	823.41615 (4.8)	396 683	823.4173(94.28)	Licoricesaponin J2	[19]

Table 1

(Continued)

No	tR (min)	Formula	Mass ion type	Found mass/error (Da, ppm)	Intensity	MS/MS ion type (m/z, area%)	Identification	Reference
59	16.2	$C_{15}H_{12}O_5$	$[M-H]^-$	271.06218 (3.6)	60 228	271.0622(48.51),177.019(3.29),151.0039(20.52),119.0501(9.32)	Naringenin	[22,25]
60	16.4	$C_{30}H_{32}O_{12}$	$[M+HCOOH-H]^-$	629.19032 (6.1)	780 166	629.1926(19.98),583.1864(19.03),553.1755(26.27),535.1648(4.27), 431.1377(6.74),165.0558(1.65),121.0298(12.49)	Benzoylpaeoniflorin	[28,30]
61	16.7	$C_{16}H_{14}O_6$	$[M-H]^-$	301.07186 (0.3)	50 187	301.0716(40.17),286.0484(6.61),242.0581(4.23),199.0398(2.27), 174.0316(1.97),164.0111(8.2),151.0034(3.42),136.0161(2.41)	Hesperetin	[22,25]
62	16.9	$C_{42}H_{62}O_{16}$	$[M-H]^-$	821.40094 (5.4)	136 382	821.4038(93.03)	Licoricesaponin H2	[19]
63	17.1	$C_{16}H_{12}O_7$	$[M-H]^-$	315.05168 (2.1)	15 776	315.0519(45.05),300.0285(34.72),271.027(1.45),151.0035(2.48)	Rhamnetin	[22,25]
64	17.1	$C_{48}H_{78}O_{18}$	$[M+HCOOH-H]^-$	987.52163 (5.8)	7260	987.5264(27.69),941.5215(33.8)	Saikosaponin N	[19,31]
65	17.3	$C_{48}H_{72}O_{21}$	$[M-H]^-$	983.45597 (6.7)	431 085	983.4592(84.78),821.4043(2.07)	Licoricesaponin A3	[19]
66	17.3	$C_{44}H_{70}O_{14}$	$[M+HCOOH-H]^-$	867.47895 (6.1)	33 250	867.4823(19.61),821.4772(65.23),779.4666(4.16),617.4106(1.9)	2''-O-Acetylsaikosaponin A	[19,27,31]
67	17.4	$C_{15}H_{12}O_4$	$[M-H]^-$	255.06643 (0.6)	140 112	255.0652(33.32),135.0078(23.85),119.0496(32.13),91.0186(4.79)	Isoliquiritigenin	[24]
68	17.9	$C_{26}H_{34}O_9$	$[M-H]^-$	489.21492 (3.9)	56 600	489.2159(69.3),471.2056(4.62),411.1849(1.14),333.136(3.46)	Deacetylnomilinic acid	[19]
69	18	$C_{26}H_{30}O_8$	$[M-H]^-$	469.18845 (3.5)	115 244	469.1904(64.66),381.209(1.07),321.1137(1.26), 306.1268(1.99),278.1318(1.93),229.1238(3.9)	Limonin	MoNA
70	18.2	$C_{42}H_{60}O_{16}$	$[M-H]^-$	819.3865 (6.9)	588 278	819.3885(92.09),351.058(1.51)	Licoricesaponin E2	[19]
71	18.2	$C_{16}H_{12}O_4$	$[M-H]^-$	267.06764 (5.1)	82 641	267.0679(28.82),252.0441(41.25),223.0409(8.71), 208.0537(1.37),195.0456(3.85),132.0219(1.53)	Formononetin	MoNA
72	18.5	$C_{48}H_{78}O_{17}$	$[M+HCOOH-H]^-$	971.52894 (8.2)	62 794	971.5333(35.95),925.5276(51.82)	Saikosaponin C	[19,27]
73	19	$C_{48}H_{80}O_{17}$	$[M+HCOOH-H]^-$	973.54486 (8.4)	78 762	973.5474(33.87),927.5411(53.18)	Saikosaponin F	[27,31]
74	19.1	$C_{42}H_{68}O_{13}$	$[M+HCOOH-H]^-$	825.46701 (4.7)	3330	825.4344(54.08),779.4655(25.1),617.4102(1.38),531.226(2.05)	Saikosaponin G	[19,32]
75	19.2	$C_{44}H_{70}O_{14}$	$[M+HCOOH-H]^-$	867.4778 (4.8)	1665	867.4646(30.15),821.4788(35.4),779.4651(8.4),761.4575(8.3)	6''-O-Acetylsaikosaponin D	[19,27,31]
76	19.2	$C_{28}H_{36}O_{10}$	$[M-H]^-$	531.22547 (3.6)	777 430	531.2269(24.5),489.2161(9.17),471.2056(19.5),427.2153(14.9), 369.1727(1.54),325.182(5.86),307.1715(1.61),59.0162(8.32)	Nomilinic acid	[19]
77	19.3	$C_{50}H_{76}O_{21}$	$[M-H]^-$	1011.48642 (5.7)	14 179	1011.4937(85.65),965.4872(1.82)	Licoricesaponin D3	[19]
78	19.4	$C_{42}H_{62}O_{17}$	$[M-H]^-$	837.39776 (7.6)	1E + 06	837.3987(89.78),351.0587(1.3)	Licoricesaponin G2	[19]
79	19.5	$C_{48}H_{78}O_{17}$	$[M+HCOOH-H]^-$	971.52917 (8.4)	31 820	971.5367(35.81),925.5299(51.93)	Saikosaponin I	[19]
80	19.7	$C_{30}H_{46}O_4$	$[M-H]^-$	469.33232 (0)	5790	469.3338(86.75),425.342(2.91)	Glycyrrhetic acid[a]	Standard
81	19.8	$C_{44}H_{70}O_{14}$	$[M+HCOOH-H]^-$	867.48079 (8.2)	2952	867.4817(21.88),821.4757(54.01),779.4633(4.33),761.4585(2.96)	4''-O-Acetylsaikosaponin D	[19,27,31]
82	20	$C_{42}H_{62}O_{16}$	$[M-H]^-$	821.40193 (6.6)	5E + 06	821.4028(63.03)	Glycyrrhizic acid[a]	Standard
83	20.2	$C_{21}H_{20}O_6$	$[M-H]^-$	367.11999 (3.5)	260 124	367.1203(54.91),352.0961(1.14),337.072(1.21), 309.0413(23.16),297.041(5.97),284.0325(2.02)	Glycycoumarin	[19]
84	20.3	$C_{42}H_{68}O_{12}$	$[M+HCOOH-H]^-$	809.474 (7.2)	4086	809.4308(31.17),763.4704(34.96),601.4143(1.07)	Saikosaponin E	[19,27]
85	20.3	$C_{36}H_{58}O_8$	$[M+HCOOH-H]^-$	663.41452 (6.4)	7032	663.4158(64.23),617.4105(23.11),595.2866(1.89)	Prosapogenin D	[19,31]
86	20.5	$C_{44}H_{70}O_{14}$	$[M+HCOOH-H]^-$	867.4801 (7.4)	9325	867.4827(14.19),821.4787(53.3),779.4686(3.1)	6''-O-Acetylsaikosaponin A	[19,27,31]
87	20.6	$C_{42}H_{64}O_{15}$	$[M-H]^-$	807.42253 (6.5)	104 728	807.4245(93.59)	Licoricesaponin B2	[19]
88	21.1	$C_{42}H_{68}O_{13}$	$[M+HCOOH-H]^-$	825.46897 (7.1)	124 814	825.473(14.36),779.4668(78.37),617.4126(2.9)	Saikosaponin A[a]	Standard
89	21.3	$C_{44}H_{70}O_{14}$	$[M+HCOOH-H]^-$	867.48045 (7.8)	17803	867.4866(22.06),821.4811(63.89),779.4676(3.83), 761.4592(2.22),617.4105(1.77)	4''-O-Acetylsaikosaponin A	[19,27,31]
90	21.3	$C_{42}H_{68}O_{13}$	$[M+HCOOH-H]^-$	825.46942 (7.7)	133 573	825.4737(17.65),779.4669(75.01),617.4098(2.75)	Saikosaponin D[a]	Standard
91	21.6	$C_{26}H_{30}O_7$	$[M-H]^-$	453.19311 (2.7)	29 642	453.1941(67.73),383.1887(2.22),365.2146(3.89),347.2026(1.44), 339.1981(1.02),316.9494(1.2),248.9613(1.28)	Obacunon	[19]
92	21.6	$C_{21}H_{18}O_6$	$[M-H]^-$	365.10352 (1.3)	14 666	365.104(49.32),350.0819(1.05),335.0566(1.59), 307.0257(26.84),295.0257(11.94),282.0183(2.89)	Neoglycyrol	[19]
93	21.7	$C_{44}H_{70}O_{14}$	$[M+HCOOH-H]^-$	867.48006 (7.4)	18 309	867.4828(20.08),821.475(36.04),779.4642(14.25),761.4539(9.79)	3''-O-Acetylsaikosaponin A	[19,27,31]
94	21.9	$C_{44}H_{70}O_{14}$	$[M+HCOOH-H]^-$	867.48111 (8.6)	5104	867.4821(21.43),821.476(41.52),779.4672(13.86), 761.4576(9.99),617.4113(1.94)	3''-O-Acetylsaikosaponin D	[19,27,31]
95	22	$C_{42}H_{62}O_{15}$	$[M-H]^-$	805.40463 (3.8)	6462	805.4088(51.55),745.5643(17.95),351.058(1.56),281.2494(1.8)	Licoricesaponin C2	[19]
96	22.1	$C_{42}H_{68}O_{13}$	$[M+HCOOH-H]^-$	825.46946 (7.7)	19 368	825.4716(18.16),779.4662(73.53),617.4112(2.8)	Saikosaponin B1	[19,32]
97	22.2	$C_{36}H_{58}O_8$	$[M+HCOOH-H]^-$	663.41327 (4.5)	7284	663.4172(74.23),617.4116(20.41)	Prosapogenin F	[19,31]
98	22.6	$C_{36}H_{58}O_8$	$[M+HCOOH-H]^-$	663.41373 (5.2)	4966	663.4176(72.72),617.4115(21.88)	Prosapogenin G	[19,31]
99	23.2	$C_{44}H_{70}O_{14}$	$[M+HCOOH-H]^-$	867.48032 (7.7)	8705	867.4853(21.02),821.48(66.14),779.4696(3.73), 761.4582(2.62),617.4126(1.36)	2''-O-Acetylsaikosaponin D	[19,27,31]
100	23.3	$C_{42}H_{68}O_{13}$	$[M+HCOOH-H]^-$	825.46958 (7.9)	11 046	825.4758(18.34),779.4691(73.92),617.4117(2.88)	Saikosaponin B2	[19,32]

MoNA, MassBank of North America, https://mona.fiehnlab.ucdavis.edu/.

[a]Verified by corresponding standard.

Table 2

Identification of chemical compounds of Si-Ni-San in positive ion mode by UPLC-Q-TOF-MS/MS

No.	tR (min)	Formula	Mass ion type	Found mass/error (Da, ppm)	Intensity	MS/MS ion type (m/z, area%)	Identification	Reference
1	2.5	$C_9H_{13}NO_2$	$[M+H]^+$	168.10144 (−2.7)	95 219	150.0908(40.33),135.0677(20.67)119.0484(3.89),107.0497(13.04)	Synephrine[a]	Standard
2	2.59	$C_{16}H_{24}O_{10}$	$[M+NH4]^+$	394.16955 (−3.1)	69 129	215.0915(5.43),201.9558(4.09),197.0807(6.93),179.0687(16.79), 151.0743(10.87),133.0653(3.32),105.0693 (1.69)	Desbenzoylpaeoniflorin	[23]
3	2.61	$C_{10}H_{13}N_5O_4$	$[M+H]^+$	268.10308 (−3.5)	259 886	268.1041(11.15),136.0612(85.64),119.0349(2.01)	Adenosine	[23]
4	2.94	C_8H_8O	$[M+H]^+$	121.06489 (0.8)	131 005	121.0654(55.73),103.0554(38.88),102.0466(3.18)	Phenylacetaldehyde	MoNA
5	3.46	$C_7H_6O_5$	$[M+H]^+$	171.02844 (−2.1)	28 648	171.0275(5.06),153.0179(26.43),135.0077(1.91),127.0388(10.57), 125.0233(13.41),109.029(20.8),107.0131 (21.1)	Gallic acid	[21,23]
6	5.4	$C_{23}H_{28}O_{12}$	$[M+H]^+$	497.16579 (0.9)	10 695	497.1605(10.24),335.1111(16.65),265.0673(2.79),197.0803(27.69), 179.067(3.98),151.0769(3.32),133.0648 (2.91),121.0284(21.11)	Oxypaeoniflorin	[23]
7	6.01	$C_{15}H_{14}O_6$	$[M+H]^+$	291.08654 (0.8)	6235	291.0834(20.32),207.0611(5.91),169.0507(3.2),161.0571(4.17), 151.0348(4.04),147.0438(4.48),139.0389 (30.99),123.0448(15.03)	Catechin	[23]
8	6.33	$C_{16}H_{18}O_9$	$[M+H]^+$	355.10231 (−0.1)	11 007	355.0617(14.7),266.9979(4.11),250.9658(3.19),193.0468(28.32), 163.0368(40.17),145.0273(2.42),135.0435 (2.34)	Chlorogenic acid	MoNA
9	6.67	C_7H_6O	$[M+H]^+$	107.04985 (6.7)	62 920	107.0503(96.36)	Benzaldehyde	,MoNA[22]
10	8.19	$C_9H_8O_4$	$[M+H]^+$	181.04957 (0.2)	5768	163.0383(41.47),145.0276(14.22),135.0433(21.87), 117.0326(15.57),107.0488(6.87)	Caffeic acid	[22]
11	9.09	$C_{23}H_{28}O_{11}$	$[M+H]^+$	481.17086 (0.9)	110 5052	481.1718(6.41),319.1184(16.2),301.1073(6.6),197.0806(26.97), 179.07(3.5),151.0754(5.7),133.0652 (5.5),105.0344(23.7)	Albiflorin[a]	Standard
12	9.09	$C_{17}H_{18}O_6$	$[M+H]^+$	319.11791 (0.9)	148 038	319.1171(9.03),301.1047(3.19),197.0803(15.17),179.0693(2.77), 151.0742(9.61),133.0646(4.77),105.0699 (3.06),105.0335(47.82)	Paeoniflorigenone	[19]
13	9.26	$C_{16}H_{18}O_9$	$[M+H]^+$	355.10291 (1.5)	7174	355.0713(7.74),266.9968(2.24),193.0486(75.18)	Cryptochlorogenic acid	MoNA
14	10.17	$C_{26}H_{28}O_{14}$	$[M+H]^+$	565.15557 (0.7)	39 729	565.1555(23.66),547.1444(9.9),529.1337(5.21),511.1222(4.99), 499.1234(3.14),427.1025(5.66),409.0922 (4.87),379.0818(3.93)	Schaftoside	[24]
15	10.33	$C_{23}H_{28}O_{11}$	$[M+NH4]^+$	498.19733 (0.7)	965 867	498.1974(6.19),301.1078(6.98),197.0809(7),179.0696(54.15), 161.0595(1.95),151.0752(10.48),135.0802 (1.28),133.0647(2.84)	Paeoniflorin[a]	Standard
16	11.52	$C_{26}H_{30}O_{13}$	$[M+H]^+$	551.17616 (0.4)	104 962	419.1342(1.74),257.0817(94.47)	Liquiritin apioside	[24]
17	11.64	$C_{21}H_{22}O_9$	$[M+H]^+$	419.13392 (0.6)	118 484	257.0814(88.66),239.0696(1.53),147.0441(1.54),137.0238(3.88)	Liquiritin[a]	Standard
18	11.8	$C_{27}H_{30}O_{16}$	$[M+H]^+$	611.16093 (0.4)	14 456	611.1829(21.48),465.1036(8),356.0669(11.2),355.0661(5.99), 303.0501(22.69),267.0021(3.12),221.0859 (2.99)	Rutin	MoNA
19	12.05	$C_{10}H_8O_3$	$[M+H]^+$	177.05449 (−0.8)	141 269	177.0545(13.63),149.0601(9.95),145.0281(31.4),134.0352(6.47), 117.0338(34.26),106.0411(2.4),103.0554 (1.89)	7-Methoxycoumarin	MoNA
20	12.05	$C_{10}H_{10}O_4$	$[M+H]^+$	195.06501 (−0.9)	41 396	177.0545(32.33),149.059(6.39),145.0284(29.25),117.0337(20.4)	Ferulic acid	[22]
21	12.11	$C_{30}H_{32}O_{15}$	$[M+NH4]^+$	650.20861 (1)	76 852	650.2107(21.01),493.1348(3.74),315.0717(31.21),297.0614(8.34), 179.0699(6.2),171.0281(2.67),153.0181 (8.22)	Galloylpaeoniflorin	[23]
22	12.43	$C_{27}H_{32}O_{14}$	$[M+H]^+$	581.18631 (−0.3)	855 556	581.1879(2.37),435.1293(6.27),419.1342(6.49),401.1238(3.16), 383.1129(4.23),315.0859(2.23),273.0749 (61.99),129.0545(1.09)	Naringin[a]	Standard
23	12.74	$C_{27}H_{30}O_{14}$	$[M+H]^+$	579.17105 (0.4)	42 644	579.1705(20.21),433.1132(35.08),271.0599(42.49)	Rhoifolin	[22,25]
24	13.05	$C_{28}H_{32}O_{15}$	$[M+H]^+$	609.1817 (0.5)	17 448	609.181(21.22),463.1215(22.07),429.1197(2.5),376.1244(1.17), 355.0771(1.71),303.0834(3.15),303.0475 (4.99),301.0704(23.29)	Diosmetin-7-neohesperidoside	MoNA
25	13.08	$C_{22}H_{24}O_{11}$	$[M+H]^+$	465.13959 (1)	87 690	465.1384(1.54),303.0865(78.63),177.054(6.59),153.0175(4.39)	Hesperetin 7-O-glucoside	[25]
26	13.09	$C_{28}H_{34}O_{15}$	$[M+H]^+$	611.19651 (−0.9)	205 7125	465.1402(5.98),449.1449(6.27),431.135(4.59),413.1242(5.51), 369.0977(2.4),345.0979(3.63),303.0856 (53.25),263.055(2.06)	Hesperidin[a]	Standard
27	13.47	$C_{23}H_{28}O_{11}$	$[M+H]^+$	481.16991 (−1.1)	37 201	481.1654(23.15),319.1175(6.47),197.0796(35.38),179.0695(5.8), 161.0596(6.4),151.0755(2.52),133.0635 (5.45),105.0333(5.57)	Mudanpioside I	[23]
28	13.63	$C_{26}H_{30}O_{13}$	$[M+H]^+$	551.17637 (0.8)	191 700	551.1771(2.14),419.1344(9.5),257.0811(84.29)	Isoliquiritin apioside	[24]

Table 2

(*Continued*)

No.	tR (min)	Formula	Mass ion type	Found mass/error (Da, ppm)	Intensity	MS/MS ion type (m/z, area%)	Identification	Reference
29	14.02	$C_{21}H_{22}O_9$	$[M+H]^+$	419.13391 (0.6)	696 951	419.1349(6.25),257.0805(82.33),147.044(2.36),137.0233(3.82)	Isoliquiritin	[22]
30	14.17	$C_{23}H_{26}O_{10}$	$[M+NH4]^+$	480.18654 (0.3)	128 361	480.1832(20.72),301.1076(43.98),179.0669(4.58),151.0762(1.98), 145.0501(2.18),133.065(3.94),105.0335(12.58)	Lactiflorin	[23]
31	14.24	$C_{22}H_{22}O_9$	$[M+H]^+$	431.13448 (1.9)	702 610	431.1361(6.43),269.0806(89.06),254.0575(1.24)	Ononin	,MoNA[19]
32	14.45	$C_{21}H_{18}O_{11}$	$[M+H]^+$	447.09293 (1.7)	50 421	447.0922(15.59),271.0603(80.81)	Baicalin	MoNA
33	14.78	$C_{15}H_{12}O_4$	$[M+H]^+$	257.08105 (0.8)	134 901	257.0826(45.41),242.058(1.84),239.0718(4.02),211.0767(2.9), 147.0447(9.22),137.0238(24.6),119.0493(2.99)	Liquiritigenin	[19,24,26]
34	15.05	$C_{15}H_{10}O_4$	$[M+H]^+$	255.06512 (-0.3)	18 389	255.0661(89.14),145.0271(2.17),137.0224(3.55),119.0478(1)	7,4'-Dihydroxyflavone	[26]
35	15.14	$C_{28}H_{34}O_{14}$	$[M+H]^+$	595.2034 (2.1)	104 9506	595.2053(2.49),449.1467(6.61),433.1514(6.55),415.1408(3.82), 397.1296(4.03),329.1031(2.18),287.0914 (59.11),263.0554(2.35)	Poncirin	MoNA
36	15.14	$C_{16}H_{14}O_5$	$[M+H]^+$	287.09191 (1.8)	123 504	287.0928(41.51),179.0347(1.4),161.0601(12.35), 153.0188(32.56),135.0819(1.16),133.0642(3.18)	Heraclenin	[19]
37	16.03	$C_{42}H_{64}O_{16}$	$[M+H]^+$	825.42731 (0.7)	90 790	825.4302(10.48),649.3965(9.97),473.3619(2.14),455.3534(73.9)	Licoricesaponin J2	[24]
38	16.08	$C_{22}H_{20}O_{11}$	$[M+H]^+$	461.10832 (1)	14 891	461.1073(8.71),285.0756(63.55),270.0501(10.2),257.0805(11.68)	Wogonoside	[27]
39	16.42	$C_{30}H_{32}O_{12}$	$[M+H]^+$	585.19741 (1.3)	95 138	585.1924(9.65),319.1179(27.09),301.1084(7.68),267.0854(9.01), 249.0746(5.27),197.0796(10.18),151.0736 (3.39),105.0335(11.67)	Benzoylpaeoniflorin	[28]
40	16.42	$C_{48}H_{72}O_{22}$	$[M+H]^+$	1001.46021 (1.4)	32 716	1001.4572(39.7),825.4249(5.64),649.3905(11.66), 631.3818(12.25),487.3394(7.7),469.3306(8.56)	24-Hydroxy-licorice-saponin A3	[29]
41	16.65	$C_{44}H_{64}O_{19}$	$[M+H]^+$	897.41323 (2)	129 769	897.4155(16.52),721.3813(2.39),703.3704(2.33),685.3587(1.02), 545.3494(29.79),527.3386 (41.83),509.3264(2.69)	Uralsaponin F	[29]
42	16.68	$C_{16}H_{14}O_6$	$[M+H]^+$	303.08641 (0.3)	29 234	303.0865(53.96),179.033(3.16),177.0534(11.72),153.0172(18.68), 149.0572(1.15),145.0282(4.55),117.0338(1.53)	Hesperetin	[19,22]
43	16.85	$C_{42}H_{62}O_{16}$	$[M+H]^+$	823.4129 (2.2)	26 760	823.4128(6.96),647.3795(8.79),471.3467(1.98), 455.3514(2.04),453.3376(72.42)	Licoricesaponin H2	[19,24]
44	17.21	$C_{48}H_{72}O_{21}$	$[M+H]^+$	985.46606 (2.2)	218 286	985.4669(40.04),809.4346(8.47),647.3809(3.63), 615.3911(23.16),453.3379(18.55)	Licoricesaponin A3	[21]
45	17.41	$C_{15}H_{12}O_4$	$[M+H]^+$	257.08072 (– 0.5)	57 313	257.0812(50.98),242.0642(1),239.0721(2.33),211.074(2.81), 147.044(8.34),137.0228(23.13),119.0488 (5.04),117.0339(0.58)	Isoliquiritigenin	[19,24,26]
46	17.94	$C_{26}H_{30}O_8$	$[M+H]^+$	471.20143 (0.2)	119 0423	471.2024(22.12),453.1921(2.13),427.2132(4.81),425.1981(24.6), 409.2022(1.85),407.1856(1.35),367.1916 (3.2),161.0601(3.64)	Limonin	MoNA
47	18.19	$C_{16}H_{12}O_4$	$[M+H]^+$	269.08081 (– 0.1)	82 641	269.0808(68.53),254.0563(3.69),253.0488(4.84),237.0533(3.91), 226.0619(3.51),213.0901(2.86),197.0592(3.04)	Formononetin	,MoNA[19]
48	18.61	$C_{20}H_{20}O_7$	$[M+H]^+$	373.12828 (0.3)	236 316	373.1283(50.99),358.1043(3.53),357.0966(2.03),343.0817(35.51)	Tangeretin	MoNA
49	19.21	$C_{28}H_{36}O_{10}$	$[M+H]^+$	533.23885 (1.4)	172 585	533.2399(23.37),515.228(4.3),455.2077(2.83),437.1962(1.61), 411.2161(3.44),369.2061(5.8),341.2098 (1.45),161.0592(1.64)	Nomilinic acid	[25]
50	19.27	$C_{42}H_{62}O_{17}$	$[M+H]^+$	839.40618 (0.2)	656 850	839.4074(10.97),663.3763(4.01),645.3656(3.4),627.3547(1.05), 487.3426(34.47),469.3316(38.88),451.3219(3.74)	Licoricesaponin G2	[29]
51	19.4	$C_{20}H_{20}O_8$	$[M+H]^+$	389.12285(-0.6)	103959	389.1241(57.24),374.0995(3.06),373.0911(1.44),359.0772(32.27)	5-Demethylnobiletin	[25]
52	19.9	$C_{42}H_{62}O_{16}$	$[M+H]^+$	823.41196 (1.1)	939 203	823.4118(5.9),647.3803(12.75),471.348(3.18),453.3357(73.06)	Glycyrrhizic acid[a]	Standard
53	20.13	$C_{20}H_{16}O_6$	$[M+H]^+$	353.10185 (– 0.3)	14 777	353.1015(56.44),338.0824(1.75),335.091(5.24),311.0499(2.52), 307.0963(3.2),183.079(1.29),153.0172 (4.32),128.9761(1.71)	Licoisoflavone B	[26]
54	20.17	$C_{21}H_{20}O_6$	$[M+H]^+$	369.13342 (0.4)	31 134	369.1332(39.79),313.0696(7.62),285.0745(6.97),270.05(1.71)	Glycycoumarin	[26]
55	20.31	$C_{21}H_{22}O_8$	$[M+H]^+$	403.13859 (– 0.4)	367 6447	403.1392(18.75),388.1166(13.75),373.0917(34.09), 358.07(3.18),355.0829(5.2),327.0874(4.82)	Nobiletin	[19,21]
56	20.5	$C_{42}H_{64}O_{15}$	$[M+H]^+$	809.4307 (– 1.4)	35 466	809.5887(58.11),633.3987(2.59),439.3574(12.67),184.0733(5.92)	Licoricesaponin B2	[29]
57	21.14	$C_{42}H_{68}O_{13}$	$[M+H]^+$	781.47367 (0.5)	19 514	781.5588(65.72),722.4816(5.44),598.4887(5.03), 455.3524(1.41),409.1616(2.08),184.0722(1.62)	Saikosaponin A[a]	Standard
58	21.22	$C_{20}H_{20}O_7$	$[M+H]^+$	373.12866 (1.3)	261 2140	373.1283(23.25),358.1058(12.2),343.0809(39.89),328.0581(2.48), 325.0714(3.73),300.0631(2.19),297.0763(3.94)	Sinensetin	,MoNA[19]
59	21.32	$C_{42}H_{68}O_{13}$	$[M+Na]^+$	803.45561 (0.5)	40 852	—	Saikosaponin D[a]	Standard
60	22.05	$C_{42}H_{68}O_{13}$	$[M+Na]^+$	803.45564 (0.5)	4622	803.4518(38.47),745.4828(2.91),621.4833(2.79)	Saikosaponin B1	[27]
61	23.3	$C_{42}H_{68}O_{13}$	$[M+Na]^+$	803.45496 (– 0.3)	1907	803.4543(95.35),331.0963(1.44)	Saikosaponin B2	[27]

MoNA, MassBank of North America, https://mona.fiehnlab.ucdavis.edu/.

[a]verified by corresponding standard

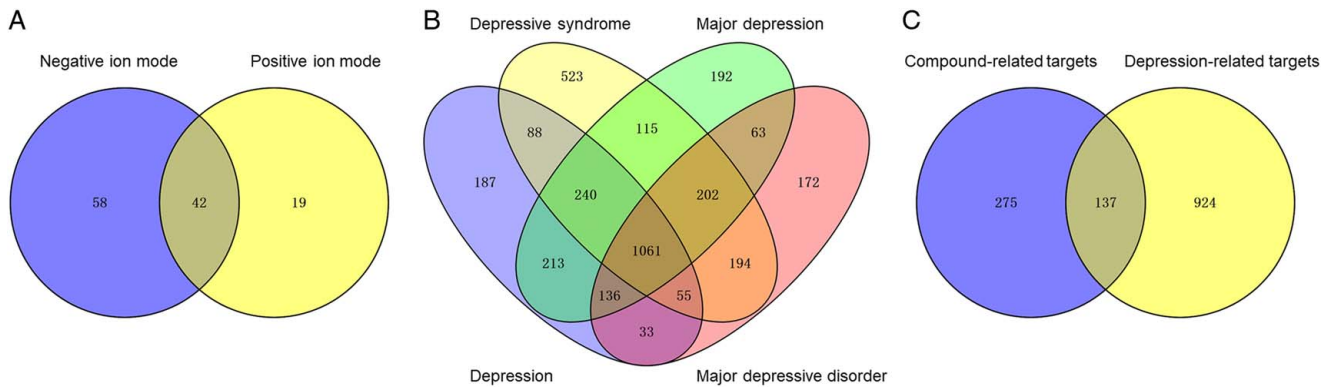

Figure 2. Venn diagrams. (A) Common compounds of Si-Ni-San in negative and positive ion mode. (B) Common depression-related targets. (C) Shared targets between compound-related targets and depression-related targets.

Discussion

Depression is a complex mental disorder. Its pathological mechanisms include neurotransmitter disorders, decreased neurogenesis, inflammation and so on[2–4]. TCM has been used to treat depression for many years, yet its pharmacological mechanisms are still elusive. Recently, with the development of computer technologies, network pharmacology is innovatively performed to study the pharmacological mechanisms of TCM for some complex diseases. Si-Ni-San has been reported to have antidepressant effect in clinical and pre-clinical studies[12–15]. However, its pharmacological mechanisms are still unclear. Thus, network pharmacology was employed to study the pharmacological mechanisms of Si-Ni-San against depression in this study. This study also met the standards of Network Pharmacology Evaluation Method Guidance, which was mainly drafted by Prof. Shao Li of Tsinghua University[20].

Table 3

Bioactive compounds of Si-Ni-San

Compounds screened out from TCMSP

No.	Compound name	Mol ID	MW	AlogP	Hdon	Hacc	Caco-2	FASA-	BBB	OB (%)	DL	TPSA	RBN
1	Albiflorin	MOL007004	480.51	−1.33	5	11	−1.52	0.35	−2.33	30.25	0.77	172.21	7
2	Baicalin	MOL002776	446.39	0.64	6	11	−0.85	0.36	−1.74	40.12	0.75	187.12	4
3	Benzoylpaeoniflorin	MOL007003	584.62	0.76	4	12	−1.35	0.4	−2.08	31.14	0.54	170.44	10
4	Catechin	MOL000492	290.29	1.92	5	6	−0.03	0	−0.73	54.83	0.24	110.38	1
5	Formononetin	MOL000392	268.28	2.58	1	4	0.78	0	0.02	69.67	0.21	59.67	2
6	Heraclenin	MOL013430	286.3	2.49	0	5	0.8	0.27	0.29	43.6	0.29	65.11	3
7	Hesperetin	MOL002341	302.3	2.28	3	6	0.37	0.33	−0.25	70.31	0.27	96.22	2
8	Lactiflorin	MOL001921	462.49	-0.57	3	10	−1.13	0.34	−1.76	49.12	0.8	140.98	5
9	Licochalcone B	MOL004841	286.3	2.88	3	5	0.47	0	−0.46	76.76	0.19	86.99	4
10	Licoisoflavone B	MOL004884	352.36	2.85	3	6	0.46	0	−0.18	38.93	0.55	100.13	1
11	Liquiritigenin	MOL001792	256.27	2.57	2	4	0.51	0.42	−0.29	32.76	0.18	66.76	1
12	Liquiritin	MOL004903	418.43	0.66	5	9	−1.06	0	−1.93	65.69	0.74	145.91	4
13	Naringenin	MOL004328	272.27	2.3	3	5	0.28	0.4	−0.37	59.29	0.21	86.99	1
14	Neoglycyrol	MOL002311	366.39	4.85	2	6	0.71	0.28	−0.2	90.78	0.67	93.04	3
15	Nobiletin	MOL005828	402.43	3.04	0	8	1.05	0.13	−0.08	61.67	0.52	85.59	7
16	Obacunon	MOL013352	454.56	2.68	0	7	0.01	0.31	−0.43	43.29	0.77	95.34	1
17	Paeoniflorigenone	MOL007016	318.35	0.79	1	6	−0.13	0.36	−0.43	65.33	0.37	82.06	4
18	Paeoniflorin	MOL001924	480.51	-1.28	5	11	−1.47	0.34	−1.86	53.87	0.79	164.37	7
19	Poncirin	MOL013276	594.62	-0.21	7	14	−1.67	0.28	−2.59	36.55	0.74	214.06	7
20	Quercetin	MOL000098	302.25	1.5	5	7	0.05	0.38	−0.77	46.43	0.28	131.36	1
21	Sinensetin	MOL001803	372.4	3.06	0	7	1.12	0.13	0.04	50.56	0.45	76.36	6

Compounds screened out from SwissADME

No.	Compound name	Mol ID	MW	Lipinski	Ghose	Veber	Egan	Muegge	BBB	GI absorption	Synthetic Accessibility	TPSA	RBN
22	5-Demethylnobiletin	Molecule 1	388.37	Yes	Yes	Yes	Yes	Yes	No	High	3.76	96.59	6
23	5-Hydroxyauranetin	Molecule 2	388.37	Yes	Yes	Yes	Yes	Yes	No	High	3.78	96.59	6
24	Epinortrachelogenin	Molecule 3	374.38	Yes	Yes	Yes	Yes	Yes	No	High	3.55	105.45	6

BBB, blood-brain barrier; DL, drug-likeness; FASA-, fractional negative accessible surface area; MW, molecular weight; OB, oral bioavailability; RBN, number of rotatable bonds; TCMSP, Traditional Chinese Medicines for Systems Pharmacology Database and Analysis Platform; TPSA, topological polar surface area.

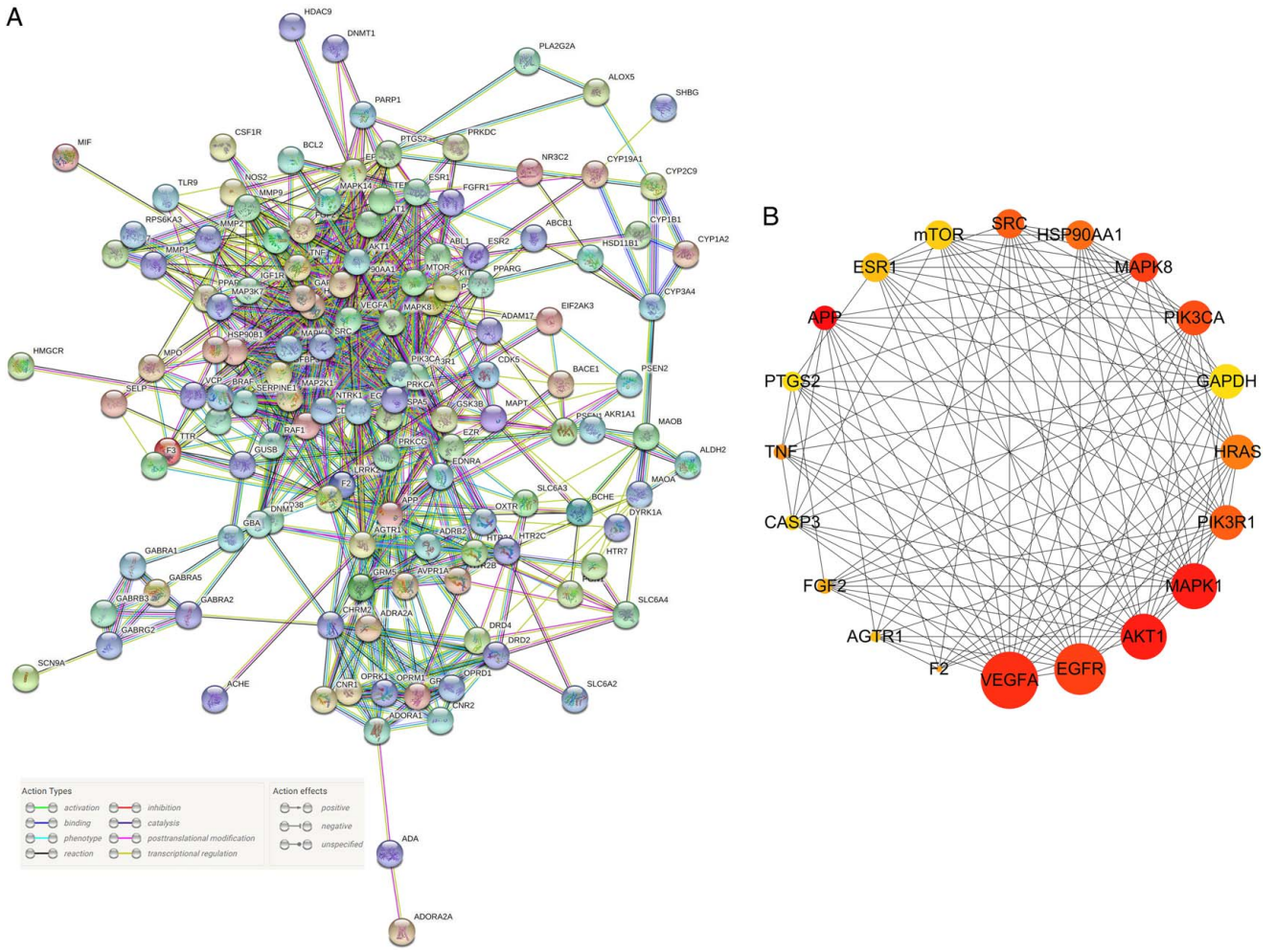

Figure 3. Protein-protein interaction (PPI) network and key targets of Si-Ni-San in the treatment of depression. (A) PPI network. Network nodes represent proteins and the edges represent protein-protein associations. (B) The top 20 targets with higher levels of degree value.

For the most studies of TCMs against depression by network pharmacology, they were performed by searching compounds from references and some TCM databases, instead of actual determined compounds[16]. However, it may be not able to clarify the actual antidepressant mechanism for TCMs. Inspired by this, our previous study performed network pharmacology of Xiang-

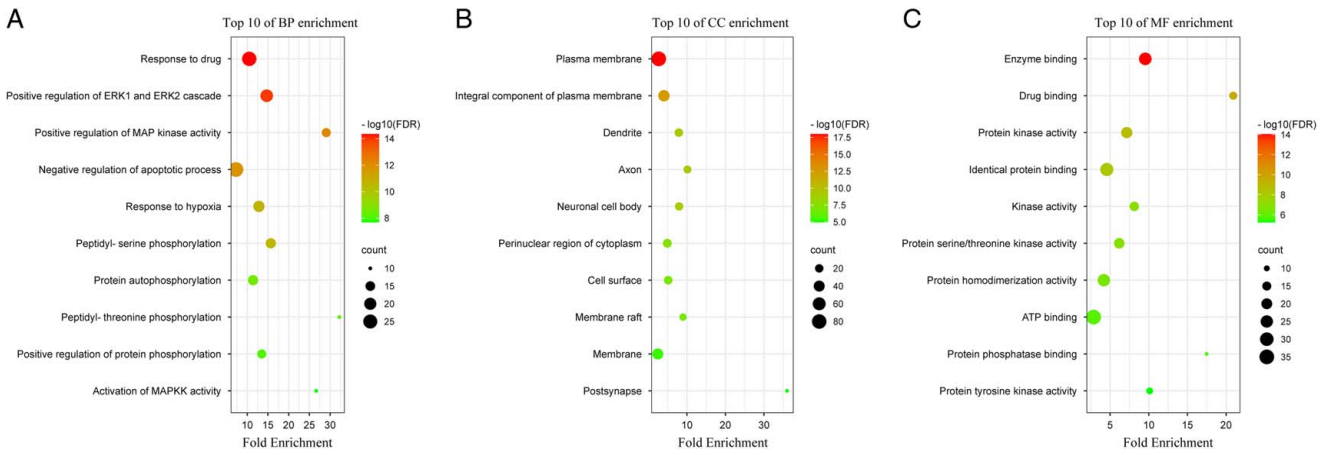

Figure 4. GO enrichment analysis of Si-Ni-San in the treatment of depression. (A) The top 10 of biological process (BP) enrichment analysis. (B) The top 10 of cell component (CC) enrichment analysis. (C) The top 10 of molecular function (MF) enrichment analysis.

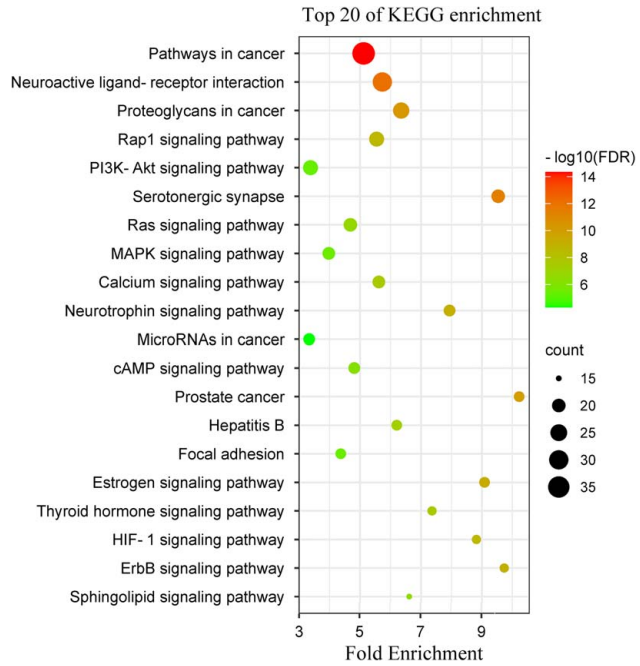

Figure 5. The top 20 of Kyoto Encyclopedia of Genes and Genomes (KEGG) pathway enrichment analysis of Si-Ni-San in the treatment of depression. FDR, false discovery rate.

Su volatile oil against menopausal depression based on the actual determined components by a method of gas chromatography-mass spectrometry. Subsequently, the antidepressant effect of Xiang-Su volatile oil was verified by metabolomics[18]. Thus, in this study, the actual determined compounds of Si-Ni-San water extract were employed by a method of UPLC-Q-TOF-MS/MS to perform the network pharmacology, which was aimed to increase the reliability and accuracy of the predicted results for the antidepressant mechanism of Si-Ni-San. Si-Ni-San water extract is reported to contain 101 compounds in negative ion mode and 21 compounds in positive ion mode by method of liquid chromatography coupled with mass spectrometry[19]. Similarly, in the present study, 100 compounds were identified in negative ion mode and 61 compounds were identified in positive ion mode. Finally, 119 compounds were left after removing the duplicates both in negative and positive ion mode. It showed that Si-Ni-San water extract mainly contained compounds of flavonoids, triterpenoid saponins, terpenoids and organic acids. Among these 119 components, 24 were considered as bioactive compounds for the antidepressant effect of Si-Ni-San after ADME screening. The bioactive components contained flavonoids like sinensetin, hesperetin, liquiritigenin, naringenin and quercetin, and terpenoids like albiflorin and paeoniflorin. More importantly, these constituents also had higher degree value in the C-T, C-T-D and C-T-P networks, which were taken as key bioactive compounds of Si-Ni-San against depression.

Furthermore, in the four herbs consisting of Si-Ni-San, sinensetin, hesperetin and naringenin are belong to *Citrus aurantium L*; liquiritigenin, naringenin and quercetin are belong to *Glycyrrhiza uralensis Fisch*; quercetin is also belong to *Bupleurum chinense DC*; albiflorin and paeoniflorin are belong to *Paeonia lactiflora Pall*. Correspondingly, most of these compounds have antidepressant action in different depressive animal models. For instance, hesperetin shows antidepressant action in a rat model of depression[40]. Naringenin improves depressive- and anxiety-like behaviours in repeated hypoxic stress-induced mice[41]. Liquiritigenin reverses depressive-like behaviour in unpredictable chronic mild stress (UCMS)-induced depressive mice[42]. Liquiritigenin is the aglycone of liquiritin, which is also verified with antidepressant effect in male and menopausal depression rats[43,44]. Quercetin alleviates depressive-like behaviours in different animal models, like stress-induced male mice[45], lipopolysaccharide (LPS)-induced male rats[46], CUMS-induced male mice[47] and oestrogen receptor α-deficient-induced female mice[48]. Albiflorin produces significant antidepressant-like effects in chronic unpredictable stress (CUS)-induced depressive rats[49] and chronic restraint stress (CRS)-induced rats[50]. Albiflorin also shows rapid antidepressant-like effects in CUMS, olfactory bulbectomy and LPS-induced murine models of depression[51]. Paeoniflorin ameliorates CRS-induced depression-like behaviours in mice[52], improves CUMS-induced depressive-like behaviours in rats[53], and alleviates CUS-induced depressive-like behaviours in rats[54]. All these results demonstrate that sinensetin, hesperetin, liquiritigenin, naringenin, quercetin, albiflorin and paeoniflorin are the key bioactive compounds for the antidepressant effect of Si-Ni-San.

In the present study, AKT1, PIK3R1, PIK3CA, mTOR, MAPK1, MAPK8 were considered as key targets for the antidepressant effect of Si-Ni-San. Among them, AKT1, PIK3R1 and PIK3CA are coding genes involved in PI3K-Akt signalling pathway, and mTOR is the downstream component of this pathway. MAPK1 and MAPK8 are coding genes of MAPK family participating in inflammation. These targets have been reported to involved in the pathogenesis of depression. For example, phosphorylated PI3K, Akt and mTOR protein levels are upregulated in hippocampus of UCMS-induced depressive mice[42]. Phosphorylated c-Jun N-terminal kinase (JNK) and p38 protein levels are increased significantly in hippocampus of CUMS-induced depressive male mice[55], indicating MAPK pathway is activated in this depressive animal model. MAPK8, also named JNK1, its mRNA expression is altered by antidepressants of nortriptyline and escitalopram in hippocampus of four inbred mouse strains using two different depressogenic protocols[56]. From all these above results, AKT1, PIK3R1, PIK3CA, mTOR, MAPK1, MAPK8 were dysregulated in depression, which could be important targets for the antidepressant effect of Si-Ni-San.

In the pathway enrichment analysis, Si-Ni-San showed its antidepressant effect by regulating pathways like PI3K-Akt signalling pathway, serotonergic synapse, MAPK signalling pathway and neurotrophin signalling pathway. Serotonin, also known as 5-hydroxytryptophan (5-HT), one of the neurotransmitters, its dysregulation is also involved in the pathogenesis of depression[57]. Brain-derived neurotrophic factor (BDNF) is a fundamental nerve growth factor in the neurotrophin signalling pathway, which is predominantly expressed in the central nervous system and related to the survival and maintenance of neuronal function. Its abnormality often causes or exacerbates the onset and progression of depression[47,49]. More importantly, the bioactive components of Si-Ni-San not only show antidepressant effect, but also regulate pathways and their related genes like PI3K-Akt, serotonergic synapse, MAPK and neurotrophin signalling pathway. For instance, Obacunon inhibits excessive cell proliferation by down-regulating mTOR and

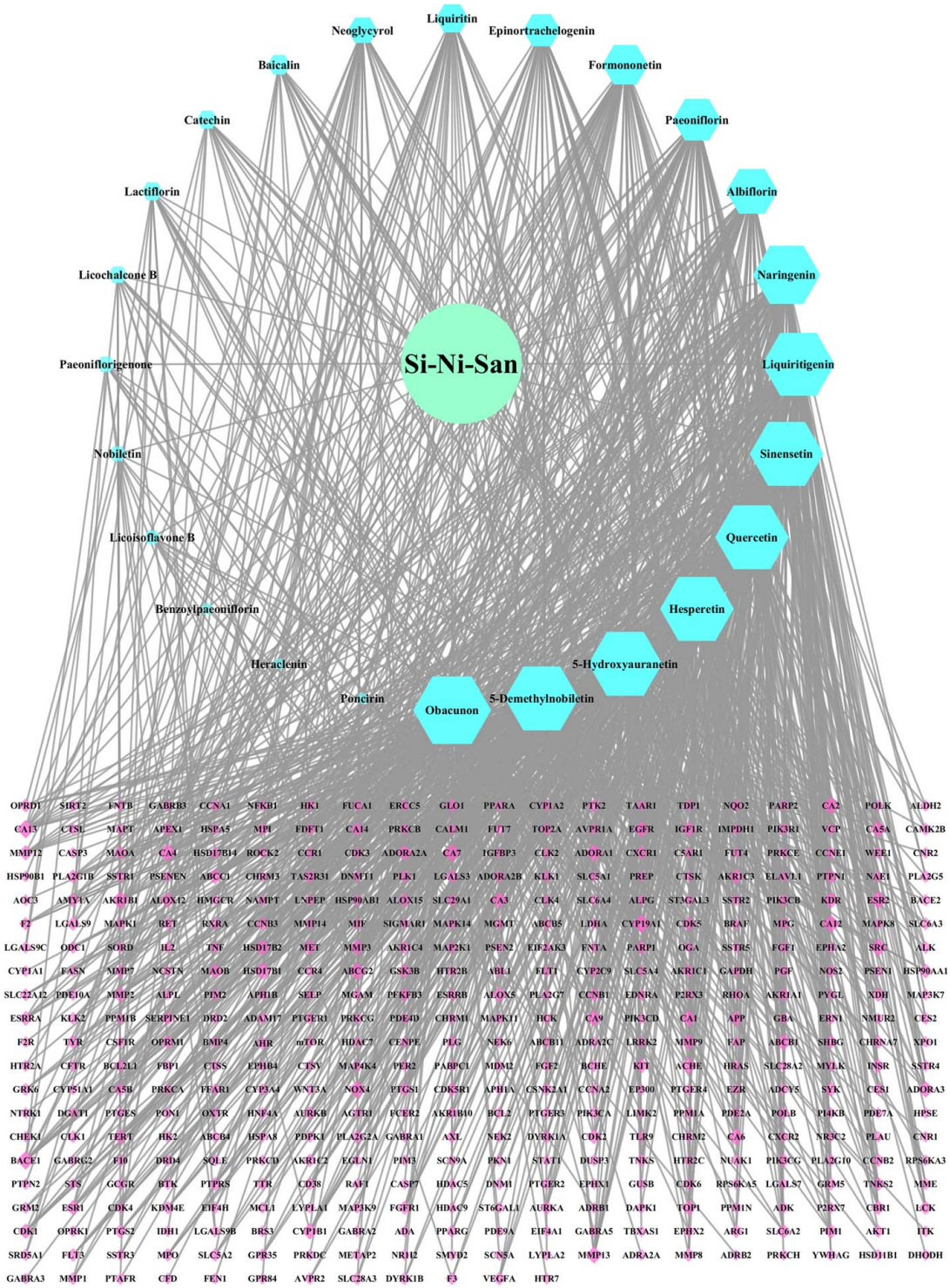

Figure 6. Compound-target (C-T) network of Si-Ni-San. Hexagons represent bioactive compounds, and diamond represents targets. Node size is proportional to its degree value. The larger the node, the more important in the network.

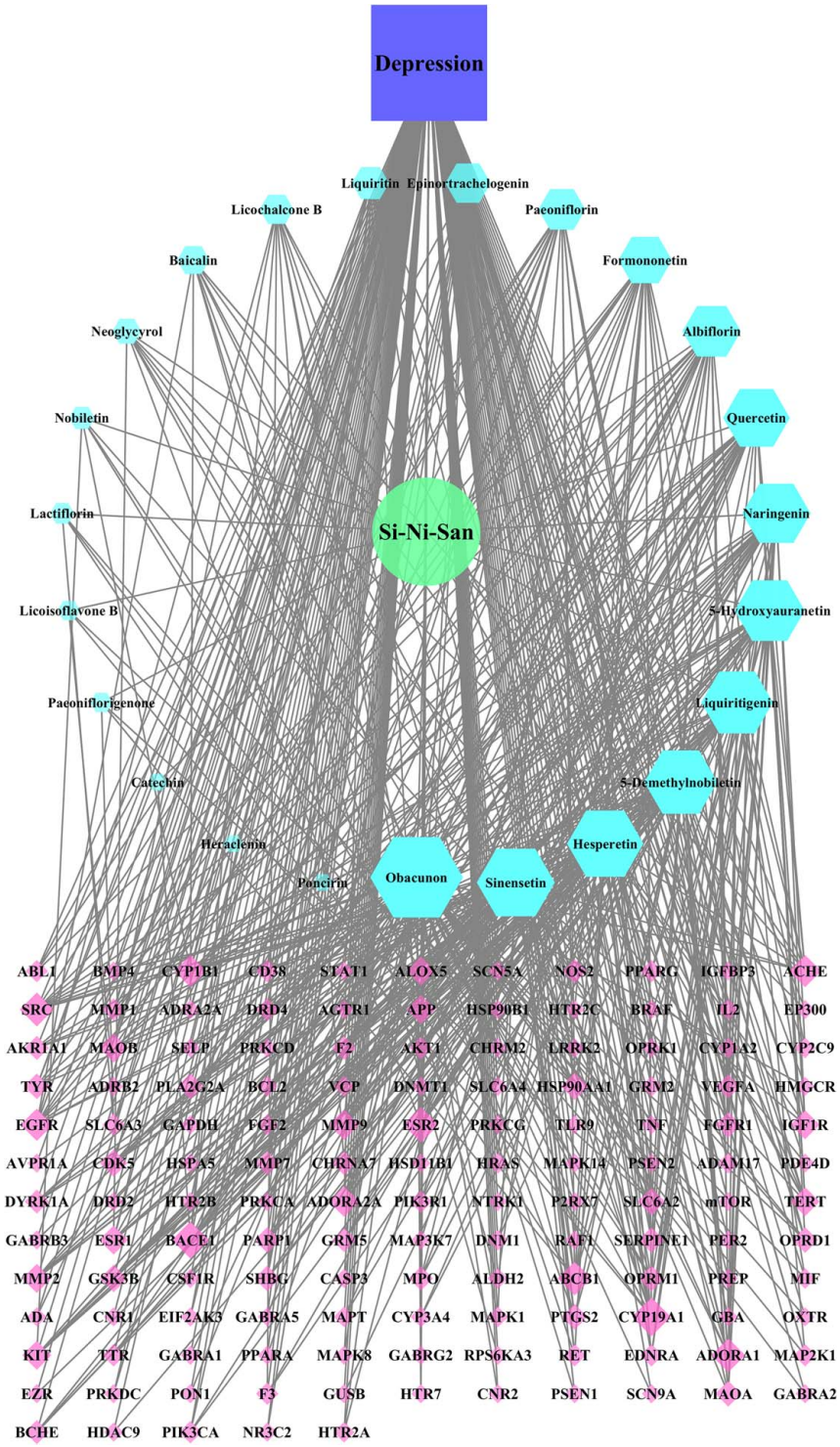

Figure 7. Compound-target-disease (C-T-D) network of Si-Ni-San against depression. Hexagon represents bioactive compounds, diamond represents targets, and square represents disease. Node size is proportional to its degree value. The larger the node, the more important in the network.

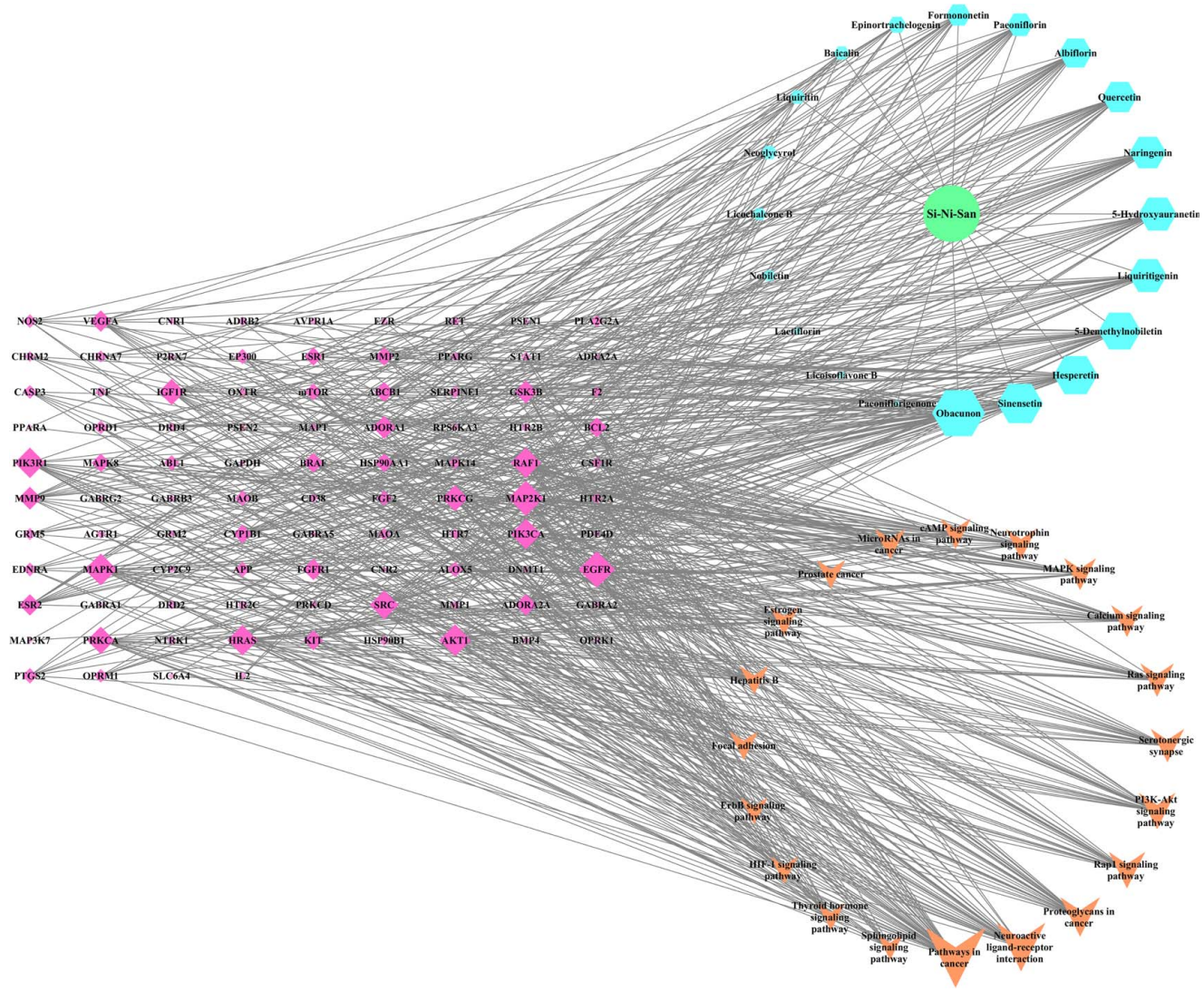

Figure 8. Compound-target-pathway (C-T-P) network of Si-Ni-San against depression. Hexagon represents bioactive compounds, diamond represents targets, and inverted triangle represents pathways. Node size is proportional to its degree value. The larger the node, the more important in the network.

MAPK signalling pathways in autosomal dominant polycystic kidney disease[58]. Sinensetin causes an effective delay in the progression of pulmonary fibrosis, and the functional mechanism is likely related to PI3K-Akt signalling by network pharmacology and in-vivo test[59]. Sinensetin also attenuates oxygen-glucose deprivation/reperfusion-induced neurotoxicity by regulating MAPK pathway in human cerebral microvascular endothelial cells[60]. Hesperetin ameliorates electroconvulsive therapy-induced memory impairment through regulation of hippocampal BDNF and oxidative stress in depressive rats[40]. Hesperetin also reduces hepatic oxidative stress and inflammation via the PI3K/Akt pathway in oleic acid-induced HepG2 cells and a rat model of high-fat diet-induced non-alcoholic fatty liver disease[61]. Liquiritigenin reverses depression-like behaviours by regulating PI3K/Akt/mTOR pathway in UCMS-induced depressive mice[42]. Naringenin improves depressive- like and anxiety-like behaviours by increasing BDNF expression in the amygdala of mice exposed to repeated hypoxic stress[41]. It also increases neuron survival in optic nerve crush injury model by inhibiting JNK-JUN pathway[62]. Quercetin protects against stress-induced anxiety-like and depression-like behaviour by regulating the serotonergic neurotransmission in mice[45], alleviates LPS-induced depressive-like behaviour via regulating BDNF in the hippocampus and prefrontal cortex in rats[46], and attenuates CUMS-induced depressive-like behaviours by promoting adult hippocampal neurogenesis including enhanced BDNF expression in mice[47]. Quercetin also exerts antidepressant effect in oestrogen receptor α-deficient female mice via BDNF-AKT/ERK1/2 signalling pathway[48], and its neuroprotective effects may be at least partly due to the inducing effects on the BDNF mRNA expression[63]. Albiflorin produces significant antidepressant-like effects by increasing the levels of 5-HT, 5-hydroxyindoleacetic acid (5-HIAA, one metabolite of 5-HT) and BDNF expression in hippocampus of CUS-induced depressive rats[49]. Albiflorin also shows antidepressant-like effects by increasing the levels of 5-HT and 5-HIAA in hippocampus, and increasing the levels of BDNF in serum and protein expression in hippocampus of CRS-induced rats[50]. It also produces rapid antidepressant-like effects by

regulating hippocampal phospholipid and tryptophan metabolism in CUMS, olfactory bulbectomy and LPS-induced murine models of depression[51]. Except the antidepressant effect, albiflorin ameliorates obesity by inducing genes like PI3K and AKT in-vivo and in-vitro tests[64]. Paeoniflorin improved intrahepatic cholestasis of pregnancy-induced ferroptosis through PI3K/AKT and MAPK signalling pathways by network pharmacology and metabolomics[65]. Paeoniflorin also promotes neurogenesis by increasing the gene transcription and protein expression of BDNF in the hippocampus dentate gyrus of CUS-induced depressive-like rats[54]. From all these results, the antidepressant mechanism of Si-Ni-San may include regulating PI3K-Akt signalling pathway, serotonergic synapse, MAPK signalling pathway and neurotrophin signalling pathway, which is benefit from the bioactive components. Finally, in order to provide a more solid scientific foundation, the above findings must be confirmed in the future through some in-vivo studies.

Conclusions

It showed that the main compounds of sinensetin, hesperetin, liquiritigenin, naringenin, quercetin, albiflorin and paeoniflorin, and main targets of AKT1, PIK3R1, PIK3CA, mTOR, MAPK1 and MAPK8 were contributed to the antidepressant effect of Si-Ni-San, which was involved in regulating PI3K-Akt signalling pathway, serotonergic synapse, MAPK signalling pathway and neurotrophin signalling pathway. Taken together, this study provides data support for the in-depth understanding of the antidepressant mechanism of Si-Ni-San by a method of UPLC-Q-TOF-MS/MS integrated with network pharmacology. Hence, Si-Ni-San may be a powerful alternative to the treatment of depression, facilitating the development of drug strategy against depression.

Ethical approval

None declared.

Consent

None declared.

Source of funding

This study was financially supported by the National Natural Science Foundation of China (Grant No. 81903823), the China Postdoctoral Science Foundation (Grant No. 2019M661903), the Jiangsu Planned Projects for Postdoctoral Research Funds, China (Grant No. 2019K163), the Priority Academic Program Development of Jiangsu Higher Education Institutions, China (PAPD), and the Open Projects of the Discipline of Chinese Medicine of Nanjing University of Chinese Medicine Supported by the Subject of Academic Priority Discipline of Jiangsu Higher Education Institutions (Grant No. ZYX03KF044).

Author contribution

K.J.: methodology, formal analysis, investigation, data curation, visualization, writing—original draft, writing—review and editing. C.L., M.X. and G.D: validation, formal analysis and resources. J.Y.Z., B.C., J.D.Z. and J.L.: investigation and visualization. Q.Z. and W.J.: conceptualization, methodology, supervision, writing—review and editing.

Conflicts of interest disclosure

The authors declare that they have no conflict of interest.

Research registration unique identifying number (UIN)

1. Name of the registry: N/A.
2. Unique Identifying number or registration ID: N/A.
3. Hyperlink to your specific registration (must be publicly accessible and will be checked): N/A.

Guarantor

Keke Jia.

Data availability statement

The figures and tables supporting the findings of this study are included within the article, and the original datasets are available from the first author or corresponding author upon request.

Provenance and peer review

Not commissioned, externally peer-reviewed.

References

[1] James SL, Abate D, Abate KH, *et al*. Global, regional, and national incidence, prevalence, and years lived with disability for 354 diseases and injuries for 195 countries and territories, 1990–2017: a systematic analysis for the Global Burden of Disease Study 2017. Lancet 2018;392:1789–858.
[2] Malhi GS, Mann JJ. Depression. Lancet 2018;392:2299–312.
[3] Sharon G, Sampson TR, Geschwind DH, *et al*. The central nervous system and the gut microbiome. Cell 2016;167:915–32.
[4] Zhang Q, Sun Y, He Z, *et al*. Kynurenine regulates NLRP2 inflammasome in astrocytes and its implications in depression. Brain Behav Immun 2020;88:471–81.
[5] Edinoff AN, Akuly HA, Hanna TA, *et al*. Selective serotonin reuptake inhibitors and adverse effects: a narrative review. Neurol Int 2021;13:387–401.
[6] Artigas F, Bortolozzi A, Celada P. Can we increase speed and efficacy of antidepressant treatments? Part I: General aspects and monoamine-based strategies. Eur Neuropsychopharm 2018;28:445–56.
[7] Xue W, Wang P, Tu G, *et al*. Computational identification of the binding mechanism of a triple reuptake inhibitor amitifadine for the treatment of major depressive disorder. Phys Chem Chem Phys 2018;20:6606–16.
[8] Yeung WF, Chung KF, Ng KY, *et al*. A systematic review on the efficacy, safety and types of Chinese herbal medicine for depression. J Psychiatr Res 2014;57:165–75.
[9] Li S, Zhang B. Traditional Chinese medicine network pharmacology: theory, methodology and application. Chin J Nat Med 2013;11:110–20.
[10] Zeng Q, Li L, Siu W, *et al*. A combined molecular biology and network pharmacology approach to investigate the multi-target mechanisms of Chaihu Shugan San on Alzheimer's disease. Biomed Pharmacother 2019;120:109370.
[11] Xie W, Meng X, Zhai Y, *et al*. Panax Notoginseng saponins: a review of its mechanisms of antidepressant or anxiolytic effects and network analysis on phytochemistry and pharmacology. Molecules 2018;23:940.
[12] Feng DD, Tang T, Lin XP, *et al*. Nine traditional Chinese herbal formulas for the treatment of depression: an ethnopharmacology, phytochemistry, and pharmacology review. Neuropsychiatr Dis Treat 2016;12:2387–402.

[13] Wang B, Lu S, Zhang C, *et al*. Quantitative proteomic analysis of the liver reveals antidepressant potential protein targets of Sinisan in a mouse CUMS model of depression. Biomed Pharmacother 2020;130:110565.
[14] Shen C, Cao K, Cui S, *et al*. SiNiSan ameliorates depression-like behavior in rats by enhancing synaptic plasticity via the CaSR-PKC-ERK signaling pathway. Biomed Pharmacother 2020;124:109787.
[15] Zong Y, Chen T, Dong H, *et al*. Si-Ni-San prevents reserpine-induced depression by inhibiting inflammation and regulating CYP450 enzymatic activity. Front Pharmacol 2019;10:1518.
[16] Shen X, Zhao Z, Luo X, *et al*. Systems pharmacology based study of the molecular mechanism of SiNiSan formula for application in nervous and mental diseases. Evid Based Complement Alternat Med 2016;2016:9146378.
[17] Chen L, Yang J, Zhao SJ, *et al*. Atractylodis rhizoma water extract attenuates fructose-induced glomerular injury in rats through anti-oxidation to inhibit TRPC6/p-CaMK4 signaling. Phytomedicine 2021;91:153643.
[18] Li Y, Yang X, Chen S, *et al*. Integrated network pharmacology and GC-MS-based metabolomics to investigate the effect of Xiang-Su volatile oil against menopausal depression. Front Pharmacol 2021;12:765638.
[19] Zhou J, Cai H, Tu S, *et al*. Identification and analysis of compound profiles of Sinisan based on 'individual herb, herb-pair, herbal formula' before and after processing using UHPLC-Q-TOF/MS coupled with multiple statistical strategy. Molecules 2018;23:3128.
[20] Li S. Network pharmacology evaluation method guidance-Draft. World J Tradition Chinese Med 2021;0:0.
[21] Wishart DS, Feunang YD, Marcu A, *et al*. HMDB 4.0: the human metabolome database for 2018. Nucleic Acids Res 2018;46(D1):D608–17.
[22] Sawada Y, Nakabayashi R, Yamada Y, *et al*. RIKEN tandem mass spectral database (ReSpect) for phytochemicals: a plant-specific MS/MS-based data resource and database. Phytochemistry 2012;82:38–45.
[23] Tan SY, Xiao X, Piao SH, *et al*. Analysis and identification of water-soluble components of Paeonia lactiflora. J Chinese Med Mater 2017;40:94–100.
[24] Zhao YM, Liu SX, Zhang CX, *et al*. Analysis on chemical constituents from Glycyrrhizae Radix et Rhizoma by HPLC-Q-TOF-MS. Chinese Traditional and Herbal. Drugs 2016;47:2061–8.
[25] Xiao F, Peng H, Xu J, *et al*. HPLC fingerprint and LC-MS chemical constituents analysis of Dalitong granules. J Chinese Med Mater 2019;42:828–34.
[26] Fang S, Qu Q, Zheng Y, *et al*. Structural characterization and identification of flavonoid aglycones in three Glycyrrhiza species by liquid chromatography with photodiode array detection and quadrupole time-of-flight mass spectrometry. J Sep Sci 2016;39:2068–78.
[27] Yang Y, Tang Y, Fan C, *et al*. Identification and determination of the saikosaponins in Radix bupleuri by accelerated solvent extraction combined with rapid-resolution LC-MS. J Sep Sci 2010;33:1933–45.
[28] Sun DD, Xu XF, Cui JC, *et al*. Analysis on chemical components from water extract of Paeoniae Radix Alba by high performance liquid chromatography-electrospray ionization-quadrupole-time of flight-mass spectrometry. China J Chinese Mater Med 2013;38:1760–5.
[29] Duan WP, Li YA, Zheng YF, *et al*. Analysis of water-soluble components in raw and honey-roasted licorice based on LC-MS/MS. Chinese Traditional Patent. Medicine 2020;42:1237–43.
[30] Shi YH, Zhu S, Ge YW, *et al*. Characterization and quantification of monoterpenoids in different types of peony root and the related Paeonia species by liquid chromatography coupled with ion trap and time-of-flight mass spectrometry. J Pharm Biomed Anal 2016;129:581–92.
[31] Sun J, Zhang LF, Fan B, *et al*. LC-MS analysis of saponins in Bupleurum Chinense DC. Chinese J Pharmacovig 2012;9:725–7.
[32] Chen WB, Shi Y, Ma YN, *et al*. Analysis of the chemical constituents of Bupleurum saponins in Bupleuri radix with turtle blood by UPLC/Q-TOF-MS/MS. Mod Food Sci Technol 2019;35:247–53.
[33] Ru J, Li P, Wang J, *et al*. TCMSP_ a database of systems pharmacology for drug discovery from herbal medicines. J Cheminform 2014;6:13.
[34] Zhang W, Zhou Q, Chen X, *et al*. Exploring potential pharmacological mechanisms of Yiqi Tuomin Decoction in the treatment of allergic rhinitis utilizing network pharmacology prediction and molecular docking-based strategies: experimental research. Ann Med Surg (Lond) 2023;85:2662–76.
[35] Daina A, Michielin O, Zoete V. SwissADME: a free web tool to evaluate pharmacokinetics, drug-likeness and medicinal chemistry friendliness of small molecules. Sci Rep 2017;7:42717.
[36] Daina A, Michielin O, Zoete V. SwissTargetPrediction: updated data and new features for efficient prediction of protein targets of small molecules. Nucleic Acids Res 2019;47(W1):W357–64.
[37] Stelzer G, Rosen N, Plaschkes I, *et al*. The GeneCards suite: from gene data mining to disease genome sequence analyses. Curr Protoc Bioinformatics 2016;54:1.30.1–33.
[38] Szklarczyk D, Gable AL, Lyon D, *et al*. STRING v11: protein-protein association networks with increased coverage, supporting functional discovery in genome-wide experimental datasets. Nucleic Acids Res 2019;47(D1):D607–13.
[39] Huang DW, Sherman BT, Lempicki RA. Systematic and integrative analysis of large gene lists using DAVID bioinformatics resources. Nat Protoc 2009;4:44–57.
[40] Alizadeh Makvandi A, Khalili M, Roghani M, *et al*. Hesperetin ameliorates electroconvulsive therapy-induced memory impairment through regulation of hippocampal BDNF and oxidative stress in a rat model of depression. J Chem Neuroanat 2021;117:102001.
[41] Olugbemide AS, Ben-Azu B, Bakre AG, *et al*. Naringenin improves depressive- and anxiety-like behaviors in mice exposed to repeated hypoxic stress through modulation of oxido-inflammatory mediators and NF-kB/BDNF expressions. Brain Res Bull 2021;169:214–27.
[42] Tao W, Dong Y, Su Q, *et al*. Liquiritigenin reverses depression-like behavior in unpredictable chronic mild stress-induced mice by regulating PI3K/Akt/mTOR mediated BDNF/TrkB pathway. Behav Brain Res 2016;308:177–86.
[43] Yang J, Jin W, Liu D, *et al*. Enhanced pseudotargeted analysis using a segment data dependent acquisition strategy by liquid chromatography-tandem mass spectrometry for a metabolomics study of liquiritin in the treatment of depression. J Sep Sci 2020;43:2088–96.
[44] Lan XY, Yu H, Chen QJ, *et al*. Effect of liquiritin on neuroendocrine-immune network in menopausal rat model. Phytother Res 2020;34:2665–74.
[45] Samad N, Saleem A, Yasmin F, *et al*. Quercetin protects against stress-induced anxiety- and depression-like behavior and improves memory in male mice. Physiol Res 2018;67:795–808.
[46] Fang K, Li HR, Chen XX, *et al*. Quercetin alleviates LPS-induced depression-like behavior in rats via regulating BDNF-related imbalance of copine 6 and TREM1/2 in the hippocampus and PFC. Front Pharmacol 2019;10:1544.
[47] Ma ZX, Zhang RY, Rui WJ, *et al*. Quercetin alleviates chronic unpredictable mild stress-induced depressive-like behaviors by promoting adult hippocampal neurogenesis via FoxG1/CREB/ BDNF signaling pathway. Behav Brain Res 2021;406:113245.
[48] Wang G, Li Y, Lei C, *et al*. Quercetin exerts antidepressant and cardioprotective effects in estrogen receptor alpha-deficient female mice via BDNF-AKT/ERK1/2 signaling. J Steroid Biochem Mol Biol 2021;206:105795.
[49] Wang YL, Wang JX, Hu XX, *et al*. Antidepressant-like effects of albiflorin extracted from Radix paeoniae Alba. J Ethnopharmacol 2016;179:9–15.
[50] Zhu Y-L, Wang L-Y, Zhao D-P, *et al*. Antidepressant-like effects of albiflorin involved the NO signaling pathway in rats model of chronic restraint stress. Chin J Nat Med 2020;18:872–80.
[51] Wang QS, Yan K, Li KD, *et al*. Targeting hippocampal phospholipid and tryptophan metabolism for antidepressant-like effects of albiflorin. Phytomedicine 2021;92:153735.
[52] Tang M, Chen M, Li Q. Paeoniflorin ameliorates chronic stress-induced depression-like behavior in mice model by affecting ERK1/2 pathway. Bioengineered 2021;12:11329–41.
[53] Zhong X, Li G, Qiu F, *et al*. Paeoniflorin ameliorates chronic stress-induced depression-like behaviors and neuronal damages in rats via activation of the ERK-CREB pathway. Front Psychiatry 2018;9:772.
[54] Chen LB, Qiu FM, Zhong XM, *et al*. Promoting neurogenesis in hippocampal dentate gyrus of chronic unpredictable stress-induced depressive-like rats with paeoniflorin. J Integr Neurosci 2019;18:43–9.
[55] Su WJ, Zhang Y, Chen Y, *et al*. NLRP3 gene knockout blocks NF-kappaB and MAPK signaling pathway in CUMS-induced depression mouse model. Behav Brain Res 2017;322(Pt A):1–8.
[56] Malki K, Lourdusamy A, Binder E, *et al*. Antidepressant-dependent mRNA changes in mouse associated with hippocampal neurogenesis in a mouse model of depression. Pharmacogenet Genomics 2012;22:765–76.
[57] Pu J, Liu Y, Gui S, *et al*. Metabolomic changes in animal models of depression: a systematic analysis. Mol Psychiatry 2021;26:7328–36.
[58] Qiu Z, He J, Shao G, *et al*. Obacunone retards renal cyst development in autosomal dominant polycystic kidney disease by activating NRF2. Antioxidants (Basel) 2021;11:38.
[59] Xu Y, Hang WL, Zhou XM, *et al*. Exploring the mechanism whereby sinensetin delays the progression of pulmonary fibrosis based on network pharmacology and pulmonary fibrosis models. Front Pharmacol 2021;12:693061.

[60] Yang D, Yang R, Shen J, *et al*. Sinensetin attenuates oxygen-glucose deprivation/reperfusion-induced neurotoxicity by MAPK pathway in human cerebral microvascular endothelial cells. J Appl Toxicol 2022;42:683–93.
[61] Li J, Wang T, Liu P, *et al*. Hesperetin ameliorates hepatic oxidative stress and inflammation via the PI3K/AKT-Nrf2-ARE pathway in oleic acid-induced HepG2 cells and a rat model of high-fat diet-induced NAFLD. Food Funct 2021;12:3898–918.
[62] Chen J, Li H, Yang C, *et al*. Citrus naringenin increases neuron survival in optic nerve crush injury model by inhibiting JNK-JUN pathway. Int J Mol Sci 2021;23:385.
[63] Rahvar M, Owji AA, Mashayekhi FJ. Effect of quercetin on the brain-derived neurotrophic factor gene expression in the rat brain. Bratisl Lek Listy 2018;119:28–31.
[64] Jeong MY, Park J, Youn DH, *et al*. Albiflorin ameliorates obesity by inducing thermogenic genes via AMPK and PI3K/AKT in vivo and in vitro. Metabolism 2017;73:85–99.
[65] Wang J, Wen J, Ma X, *et al*. Validation of MAPK signalling pathway as a key role of paeoniflorin in the treatment of intrahepatic cholestasis of pregnancy based on network pharmacology and metabolomics. Eur J Pharmacol 2022;935:175331.